The Rapid Solution of the Laplace Equation on Regions with Fractal Boundaries

J. H. Ma
Research Report YALEU/DCS/RR-927
October 21, 1992

The author was supported in part by DARPA under Grant DMS-9012751, and in part by ONR under Grant N00014-89-J-1527.
Approved for public release: distribution is unlimited.
Keywords: *Laplace Equation, Fast Algorithms, Scattering Matrix, Harmonic Measure.*

ABSTRACT

The Rapid Solution of the Laplace Equation on Regions with Fractal Boundaries

Jin Hong Ma

Yale University

1992

Interest in the numerical solution of the Laplace equation on regions with fractal boundaries arises both in mathematics and physics. In mathematics, examples include harmonic measure of fractals, complex iteration theory, and potential theory. In physics, examples include Brownian motion, crystallization, electrodeposition, viscous fingering, and diffusion-limited aggregation. In a typical application, the numerical simulation has to be on a very large scale involving at least tens of thousands of equations with as many unknowns, in order to obtain any meaningful results. Attempts to use conventional techniques have encountered insurmountable difficulties, due to excessive CPU time requirements of the computations involved. Indeed, conventional direct algorithms for the solution of linear systems require order $O(N^3)$ operations for the solution of an $N \times N-$ problem, while classical iterative methods require order $O(N^2)$ operations, with the constant strongly dependent on the problem in question. In either case, the computational expense is prohibitive for large-scale problems. We present a direct algorithm for the solution of the Laplace equation on regions with fractal boundaries. The algorithm requires $O(N)$ operations with a constant dependent only on the geometry of the fractal boundaries. The performance of the algorithm is demonstrated by numerical examples, and applications and generalizations of the scheme are discussed.

Contents

List of Tables

List of Figures

Chapter 1

Introduction

During the last decade, the numerical solution of the Laplace equation on regions with fractal boundaries has been becoming increasingly popular both in mathematics and physics. In mathematics, examples include harmonic measure of fractals, complex iteration theory, and potential theory. In physics, examples include growth phenomena such as crystallization, electrodeposition, viscous fingering, and diffusion-limited aggregation, where the harmonic measure governs the growth of the fractal surfaces [56]. Thus, much recent work has been focused on the study of the metric properties of harmonic measure on fractals [5], [12], [33], [38], and [34].

1.1 Background

Carleson proved recently in [12] that the dimension of the support of harmonic measure for any two-dimensional Cantor set is strictly less than one . However, the actual values for particular sets have not been determined, and it is unclear how they can be, without some form of computer experimentation. In R^3, the behavior of harmonic measure for Cantor sets is completely unknown. Thus, several attempts have been made during the last several years to solve such problems numerically (see [5] and [34]).

There are two approaches to the study of the metric properties of the harmonic measure on fractals.

1. Viewing the harmonic measure as the relative hitting probability at points on the surface, and using the Monto Carlo method to conduct computer simulations on parallel machines such as the Connection machine (see [5]).

2. Formulating the problem as an integral equation of the first kind, and using brute force to solve it numerically.

While the first approach has produced some significant results (see [5]), the computation becomes prohibitively expensive when high accuracy is desired, due to the slow convergence of the Monto Carlo method (as is well known, the error of a Monto Carlo simulation decays like $1/\sqrt{N}$, where N is the number of trials).

On the other hand, the second approach has also encountered insurmountable difficulties, due to excessive CPU time requirements of the computations involved. Indeed, in order to obtain mathematically meaningful results, systems of linear equations have to be solved, involving at least tens of thousands of equations with as many unknowns. Conventional direct algorithms for the solution of linear systems require order $O(N^3)$ operations for the solution of an $N \times N-$ problem, while classical iterative methods require order $O(N^2)$ operations, with the constant strongly dependent on the problem in question. In either case, the computational expense is prohibitive for large-scale problems.

We present a direct algorithm for the rapid solution of the Laplace equation on regions with a certain type of fractal boundaries. The algorithm requires $O(N)$ operations with a constant dependent only on the geometrical property of the fractal boundaries, where N is the number of elements in the discretization of the fractal. And the evaluation of the potential at any point requires $O(\log(N))$ operations.

1.2 Genealogy of Fast Algorithms

The algorithm of this thesis is closely related to other analysis-based fast algorithms. Among them, perhaps the Fast Multipole Method (FMM) [25] is the best known. It provides a fast scheme to evaluate gravitational and electrostatic potentials involving a large number of particles. In [8], wavelets are used to generalize the FMM to a variety of integral operators. In [4], wavelets are combined with the Schultz algorithm to solve integral equations of the second kind. Several other "fast" schemes have been constructed, such as the algorithm of [27] for the rapid evaluation of Gauss transforms. In [48], a fast direct solver is developed for the solution of integral equations in one dimension. However, the latter algorithm substantially exploits the one-dimensional geometry. While the algorithms of [25], [8], [4], [3], and [27] are essentially fast algorithms for applying a matrix to a vector, our algorithm can be viewed as a fast direct inversion scheme for the some of matrices of the type produced by the FMM.

1.3 Outline of the Dissertation

The direct algorithm presented in this thesis exploits the fact that far-field interactions are of low rank for any given precision, and low rank operators can be recursively compressed without actually generating them.

We begin with the definition of the problems to be addressed in Chapter 2. In Chapter 3, we summarize certain mathematical and numerical facts to be used in this thesis. In Chapter 4, we establish the principal analytical tool of this thesis that ranks of far-field interactions are finite to any given precision. In Chapter 5, we develop the mathematical apparatus used to construct the fast algorithm by borrowing terminology from the standard scattering theory for the Helmholtz equation. In Chapter 6, we present the description of the fast algorithm, and in Chapter 7, we illustrate the performance of the algorithm by numerical examples. Finally, in Chapter 8, we outline some applications and generalizations.

Chapter 2

Statement of the Problems

As is well-known, the governing equation for potential problems is the Laplace equation

$$\Delta u = \frac{\partial^2 u}{\partial x^2} + \frac{\partial^2 u}{\partial y^2} = 0. \tag{2.1}$$

Functions which satisfy (2.1) are referred to as harmonic functions.

In this chapter, we define the problems to be addressed, namely, the boundary value problems for the Laplace equation on regions with fractals of Cantor type as the boundaries.

2.1 Fractal Boundaries

A fractal of Cantor type is a classical example of fractals (see, for example, [7], [16], and [39]), which can be generated recursively by dividing a given region into four corner regions (boxes) with a ratio of sides as a parameter.

Given a real number a ($0 < a < \frac{1}{2}$), we define a sequence of sets as follows (See Figures 2.1, 2.2, and 2.3):

$$C_0^a = \{ \text{ the unit square } \}, \tag{2.2}$$

$$C_1^a = \{4 \text{ corner boxes with } a \text{ as their sizes } \}, \tag{2.3}$$

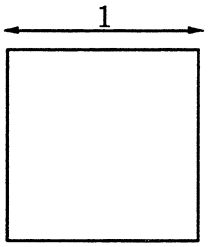

Figure 2.1: Set C_0^a

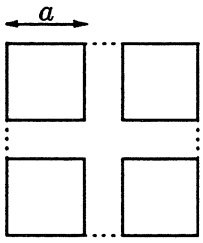

Figure 2.2: Set C_1^a

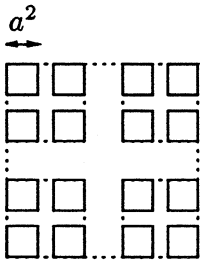

Figure 2.3: Set C_2^a

$$C_l^a = \{4^l \text{ corner boxes with } a^l \text{ as their sizes }\}, \tag{2.4}$$

where l is an integer.

The Cantor set associated with the ratio a is the limit of the sequence of sets $\{C_l^a\}$, which decreases monotonically:

$$C_0^a \supseteq C_1^a \supseteq C_2^a \supseteq \cdots.$$

The limit is defined as the intersection of the sets $\{C_l^a\}$

$$C^a = \bigcap_{l \in \{0,1,2,\ldots,\infty\}} C_l^a. \tag{2.5}$$

For a given $l \geq 1$, we will define the l-th approximation to the Cantor set (associated with the ratio a) as a set

$$A_l = \{ \text{ the centers of all boxes in } C_l^a \}. \tag{2.6}$$

We will refer to the 4^l boxes C_l^a generated during the $l - th$ step of the above process as level l boxes. Thus, there is one box on level 0, and it coincides with the unite square. The level $l+1$ is obtained from the level l by subdividing each box on the level l into 4 corner boxes (see Figure 2.2).

We will also impose a tree structure on the hierarchical structure of C^a, so that if *ibox* is a fixed box at level l, the four boxes at level $l+1$ obtained by subdivision of *ibox* are considered its children, while the four child boxes are considered neighbors.

2.2 The Laplace Equation

Let C^a denote the Cantor set associated with the given ratio a (see Figure 2.4). We will consider the following exterior Dirichlet problem for the Laplace equation

$$\begin{cases} \Delta u = 0 \quad \text{for} \quad \mathrm{x} \in R^2 \setminus C^a, \\ u|_{C^a} = f. \end{cases} \tag{2.7}$$

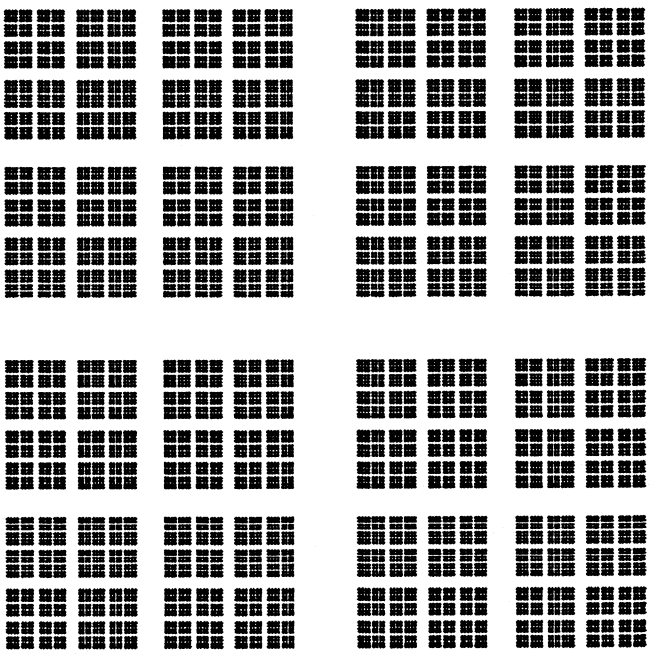

Figure 2.4: Cantor Set C^a - A Fractal

To insure the uniqueness of the solution of problem (2.7), the far-field condition

$$\lim_{r\to\infty}\left|u(\mathrm{x})-r\ln r\frac{\partial u(\mathrm{x})}{\partial r}\right|=0 \tag{2.8}$$

is normally imposed. In the above formula, $r^2=(x-x_0)^2+(y-y_0)^2$ with point $\mathrm{x}=(x,y)\in R^2\backslash C^a$ and an arbitrary fixed point $\mathrm{x}_0=(x_0,y_0)\in C^a$.

Remark 2.1 *As is well-known, for any harmonic function $u: R^2\to R^1$, there exists two functions, φ and ψ,*

$$\varphi(r,\theta)=\sum_{k=-\infty}^{\infty}\alpha_k r^{|k|}e^{ik\theta},$$

$$\psi(r,\theta)=\sum_{k=-\infty}^{\infty}\beta_k r^{|k|}e^{ik\theta}+\gamma\ln r,$$

such that $u=\varphi+\psi$.

The far-field condition (2.8) excludes the constant term in the expansion of ψ while allowing the logarithm term.

The proof of the following theorem can be found, for example, in [55].

Theorem 2.1 *The boundary value problem (2.7) with the far-field condition (2.8) is a well-posed problem.*

As is well-known (see [15], for example), the boundary value problem (2.7) with the far-field condition (2.8) can be formulated as an integral equation of the first kind by representing the solution as the logarithmic potential of the charge distribution on the boundary C^a. The charge distribution is a Borel measure on the Cantor set C^a (see [15]). Denoting by σ the charge distribution over the boundary C^a, we obtain the integral equation

$$\int_{C^a}\ln|x-t|d\sigma(t)=f(x) \tag{2.9}$$

with $x\in C^a$, where the integration is in the sense of Borel measure.

Remark 2.2 *As is well-known, the Lebesgue measure of a Cantor set C^a is zero, However, the equation (2.9) is mathematically sound due to the fact that any Cantor set C^a possesses a positive capacity (for detail, see [15] or [55])*

For a given integer $L \geq 1$, suppose that $N = 4^L$, and $A_L = \{z_i \mid i = 1, 2, \ldots, N\}$ is the L-th approximation to the Cantor set C^a. Then, by the definition of Borel integration, the integral equation (2.9) is discretized as a linear system of equations

$$A\sigma = b \quad \text{with} \quad A \in R^{N \times N} \quad \text{and} \quad b \in R^N, \tag{2.10}$$

where

$$A_{ij} = \log \mid z_i - z_j \mid \text{ for } i \neq j, \text{ and } A_{ij} = l \cdot \log a + \delta \quad \text{for } i = j. \tag{2.11}$$

In formula (2.11), δ is a constant dependent on the ratio a and the total number of levels L in the approximation of Cantor set C^a. The actual choice of the constant δ will be discussed in Chapter 7.

Given a measure μ over C^a, we define an integral operator $P_\mu : R^2 \rightarrow R^1$ by the formula

$$P_\mu(x) = \int_{C^a} \ln |x - t| d\mu(t). \tag{2.12}$$

Lemma 2.1 can very easily verified; and it states that with any non-negative measure μ over C^a, the function $P_\mu(x)$ is negative for $x \in C^a$. Theorem 2.2 is the immediate consequence of Lemma 2.1.

Lemma 2.1 *If μ is a non-negative measure over C^a, then*

$$P_\mu(x) < 0 \quad \textit{for } x \in C^a. \tag{2.13}$$

Theorem 2.2 *There exists an integer N_0 such that for any integral $N > N_0$, the coefficient matrix A in (2.10) is negative definite.*

Remark 2.3 *Experiments show that the integer N_0 in Theorem 2.2 can be as small as $N_0 = 64$ (see Chapter 7).*

Chapter 3

Mathematical and Numerical Preliminaries

In this chapter, we summarize certain well-known mathematical and numerical facts to be used in the rest of this thesis. They can be found, for example, in [10], [13], and [55].

3.1 Potential Theory for the Laplace Equation

3.1.1 Green's Function

Definition 3.1 *(**Green's function in** R^2) Suppose that $\Omega \subset R^2$ is an open connected set, then for $P \in \Omega$, function $G(z,P) : \Omega \to R^1$ will be referred to as the Green's function of Ω with pole (or singularity) at P if it satisfies the following three conditions.*

1. *$G(z,P)$ is harmonic in Ω, except at the point P.*

2. *If $P \neq \infty$, then*

$$g(z) = G(z,P) - \log|z-P| \tag{3.1}$$

is harmonic in a neighborhood of P.

If $P = \infty$, then

$$g(z) = G(z, \infty) - \log|z| \tag{3.2}$$

is harmonic in a neighborhood of ∞.

3. *As z tends to any point on the boundary of Ω, then*

$$G(z, P) \to 0. \tag{3.3}$$

Theorem 3.1 *(**Existence of Green's Function in R^2**) Suppose that $\Omega \subset R^2$ be a domain bounded by a Jordan curve Γ. Then the Green's function $G(z, P)$ for Ω exists for any $P \in \Omega$.*

Lemma 3.1 *(**Green's Formula**) Let $\gamma : [0, L] \to R^2$ be a closed Jordan curve, with image of γ denoted by Γ. Suppose that $\Omega \subset R^2$ is the interior of Γ, so that $\Gamma = \partial\overline{\Omega}$. Suppose further that $N_t : [0, L] \to R^2$ is the interior normal to Γ, function G: $\Omega \times \Omega \to R^1$ is the Green's function for Ω, and $\varphi \in L^2(\Gamma)$. Then the function $u : \Omega \to R$ defined by the formula*

$$u(x) = \frac{1}{2\pi} \int_0^L \varphi(\gamma(t)) \cdot \frac{\partial}{\partial N_t} G(x, \gamma(t)) \cdot dt \tag{3.4}$$

is harmonic, and $u|_\Gamma = \varphi$.

3.1.2 Boundary Value Problems for the Laplace Equation

Suppose that $\Gamma \subset R^2$ is a Jordan curve, parameterized by its length $\gamma : [0, L] \to R^2$, and Ω is the region bounded by Γ, so that $\partial\overline{\Omega} = \Gamma$. Suppose further that $N : [0, L] \to R^2$ is the interior normal to Γ. For an integrable function $f : [0, L] \to R^1$, we will be solving one of the following problems.

(A) Interior Dirichlet problem

$$\begin{aligned} \Delta\Phi(x) &= 0 && \text{for} \quad x \in \Omega \\ \Phi(x) &= f(\gamma^{-1}(x)) && \text{for} \quad x \in \Gamma \end{aligned} \tag{3.5}$$

(B) Exterior Neumann problem

$$\begin{aligned} \Delta\Psi(x) &= 0 && \text{for} \quad x \in R^2\backslash\Omega \\ \tfrac{\partial}{\partial N}\Psi(x) &= f(\gamma^{-1}(x)) && \text{for} \quad x \in \Gamma \end{aligned} \tag{3.6}$$

with Ψ satisfying the far-field condition (2.8).

As is well known, each of the above two problems has a unique solution for any continuous right hand side f and piecewise smooth boundary Γ (see, for example, [13]).

3.1.3 Single and Double Layer Potentials

Suppose that a point charge of unit intensity is located at the point $x_0 \in R^2$. Then, for any $x \in R^2$ with $x \neq x_0$, the potential due to this charge is described by the expression

$$\phi_{x_0}(x) = -\ln(||x - x_0||). \tag{3.7}$$

The potential of a dipole of unit intensity located at x_0 and oriented at the direction $h \in R^2$ ($||h|| = 1$) is described by the formula

$$\phi_{x_0,h}(x) = \frac{h(\mathrm{x} - \mathrm{x_0})}{||\mathrm{x} - \mathrm{x_0}||^2}. \tag{3.8}$$

For an integrable function $\mu : [0, L] \rightarrow R^1$, the potential of a single layer with density μ is given by the formula

$$\Psi(x) = \int_0^L \phi_{\gamma(t)}(x)\mu(t)dt, \tag{3.9}$$

and the potential of a double layer with the dipole density μ is given by the formula

$$\Phi(x) = \int_0^L \phi_{\gamma(t),N(t)}(x)\mu(t)dt. \tag{3.10}$$

3.1.4 Integral Equations of the Classical Potential Theory

In the classical potential theory, the interior Dirichlet problem (3.5) is solved by representing Φ as the potential of a double layer, and the exterior Neumann problem

(3.6) is solved by representing Ψ as the potential of a single layer. The analysis of the single layer and double layer potentials in the vicinity of the boundaries results in two integral equations of the second kind.

(A1) Interior Dirichlet Problem

$$\pi\mu(x) + \int_0^L \frac{\partial}{\partial N(t)} \log ||\gamma(x) - \gamma(t)||\mu(t)dt = f(x). \tag{3.11}$$

(B1) Exterior Neumann Problem

$$-\pi\mu(x) + \frac{\partial}{\partial N(x)} \int_0^L \log ||\gamma(x) - \gamma(t)||\mu(t)dt = f(x). \tag{3.12}$$

3.2 Galerkin Method for the Solution of Integral Equations

As is well-known, the classical Galerkin method can be used for the numerical solution of the integral equations of the form

$$\mu(x) + \int_a^b K(x,t)\mu(t)dt = f(x). \tag{3.13}$$

The following is the brief description of the Galerkin method.

Suppose that $\{P_1(x), P_2(x), \cdots, P_n(x), \cdots\}$ is the orthonormal basis in $L^2[a,b]$. Then the function $\mu_n : [0,L] \to R^1$ defined by the formula

$$\mu_n(x) = \sum_{j=1}^{n} \alpha_j P_j(x), \tag{3.14}$$

and satisfying the condition

$$(r, \mu_n) = 0, \tag{3.15}$$

will be used to approximate the solution of the integral equations (3.13). The error function $r(x)$ in formula (3.15) is defined via the expression

$$r(x) = \mu_n(x) + \int_0^L K(x,t)\mu_n(t)dt - f(x). \tag{3.16}$$

The above procedure results in a linear system $Bx = b$ defined by formulae

$$B_{ij} = \int_0^L \int_0^L K(x,t)P_i(t)P_j(t)dxdt \qquad i \neq j, \tag{3.17}$$

for $1 \leq i,j \leq n$, and $B_{ii} = 1$,

$$b_i = \int_0^L f(x)P_i(x)dx, \tag{3.18}$$

for $1 \leq i \leq n$.

A detailed discussion of the Galerkin method for the solution of the equations of the classical potential theory can be found, for example, in [6], [10], [14], [20], [24], [32], [52], [53], and [61].

Chapter 4

Fields of Charges

In this chapter, we investigate in some detail the structure of potential fields in R^2, and prove Theorem 4.2, which is the principal analytical tool of this thesis.

It is well known that the potential ϕ_{x_0} due to a point charge at $x_0 \in R^2$ (defined by formula (3.7)) is harmonic in any region excluding the source point x_0. Moreover, for any harmonic function $u : R^2 \to R^1$, there exists an analytic function $w : \mathbb{C} \to \mathbb{C}$ such that $u(x,y) = Re(w(x,y))$. In the rest of this thesis, we will make no distinction between points in R^2 and points in $\mathbb{C}$. In complex terms, the potentials ϕ_{x_0} and $\phi_{x_0,h}$ defined by the expressions (3.7) and (3.8) respectively, assume the form

$$\phi_{z_0}(z) = Re(-\ln(z - z_0)),$$

and

$$\phi_{z_0,h}(z) = Re(\frac{h}{z - z_0}),$$

where $z = x + iy$ and $z_0 = x_0 + iy_0$. Following the standard practice, we will refer to the analytic function $\ln(z - z_0)$ as the potential at the point $z \in \mathbb{C}$ due to a charge located at the point z_0.

4.1 Ranks of Interaction Matrices

The following lemma can be easily proved by expanding $\ln(1-\omega)$ into Taylor series with respect to ω.

Lemma 4.1 *Let a unit point charge be located at z_0. Then for any z such that $|z| > |z_0|$,*

$$\phi_{z_0}(z) = \ln(z - z_0) = a_0 \ln(z) + \sum_{k=1}^{\infty} \frac{a_k}{z^k}, \tag{4.1}$$

where

$$a_0 = 1 \qquad \text{and} \qquad a_k = (-)\frac{z_0^k}{k}. \tag{4.2}$$

Furthermore, for any $p \geq 1$,

$$\left| \phi_{z_0}(z) - a_0 \ln(z) - \sum_{k=1}^{p} \frac{a_k}{z^k} \right| \leq (\frac{1}{c-1})(\frac{1}{c})^p, \tag{4.3}$$

where

$$c = \left| \frac{z}{z_0} \right|. \tag{4.4}$$

Remark 4.1 *The above lemma can be reformulated in a slightly different way, which will be used later.*

Truncating the expansion (4.1) after p terms ($p \geq 1$), we will denote the error of the truncated expansion by $\varepsilon_{z_0}^p(z)$, so that

$$\varepsilon_{z_0}^p(z) = \phi_{z_0}(z) - a_0 \ln(z) - \sum_{k=1}^{p} \frac{a_k}{z^k}.$$

Then for any $p \geq 1$,

$$\phi_{z_0}(z) = \varepsilon_{z_0}^p(z) + u_p v_p^T \tag{4.5}$$

with the vectors u_p and v_p defined by the formulae

$$u_p = (\ln z, \frac{1}{z}, \frac{1}{z^2}, \cdots, \frac{1}{z^p}) \tag{4.6}$$

$$v_p = (1, \frac{-z_0}{1}, \frac{-z_0^2}{2}, \cdots, \frac{-z_0^p}{p}). \tag{4.7}$$

Furthermore,

$$\left|\varepsilon_{z_0}^p(z)\right| \leq \left(\frac{1}{c-1}\right)\left(\frac{1}{c}\right)^p \tag{4.8}$$

with c defined by (4.4).

Clearly, the truncation error $\varepsilon_{z_0}^p(z)$ in (4.8) decays exponentially as the function of p. Thus few terms in (4.1) are needed to achieve any given accuracy,

The following theorem is the principal analytical tool of this thesis. It states that under certain conditions, the rank of the matrix describing the potential interaction between two sets in R^2 is finite to any given precision.

We define the interaction matrix between the two sets of points $\{x_1, \cdots, x_m\}$ and $\{y_1, \cdots, y_n\}$ as a $m \times n$ matrix

$$\left(\phi_{y_j}(x_i)\right) = \begin{pmatrix} \phi_{y_1}(x_1) & \phi_{y_2}(x_1) & \cdots & \phi_{y_n}(x_1) \\ \phi_{y_1}(x_2) & \phi_{y_2}(x_2) & \cdots & \phi_{y_n}(x_2) \\ \vdots & \vdots & & \vdots \\ \phi_{y_1}(x_m) & \phi_{y_2}(x_m) & \cdots & \phi_{y_n}(x_m) \end{pmatrix} \tag{4.9}$$

$$= \begin{pmatrix} \ln(x_1 - y_1) & \ln(x_1 - y_2) & \cdots & \ln(x_1 - y_n) \\ \ln(x_2 - y_1) & \ln(x_2 - y_2) & \cdots & \ln(x_2 - y_n) \\ \vdots & \vdots & & \vdots \\ \ln(x_m - y_1) & \ln(x_m - y_2) & \cdots & \ln(x_m - y_n) \end{pmatrix}. \tag{4.10}$$

The following theorem follows immediately from formulae (4.5) and (4.8).

Theorem 4.1 *Let n unit point charges be located within the circle $|y| < R$ at points $\{y_1, y_2, \cdots, y_n\}$, $\lambda > 0$ be some real number, and $\{x_1, x_2, \cdots, x_m\}$ be another set of points such that $|x_i| > (1+\lambda)R$ for all $1 \leq i \leq m$ (see Figure 4.1). Then the*

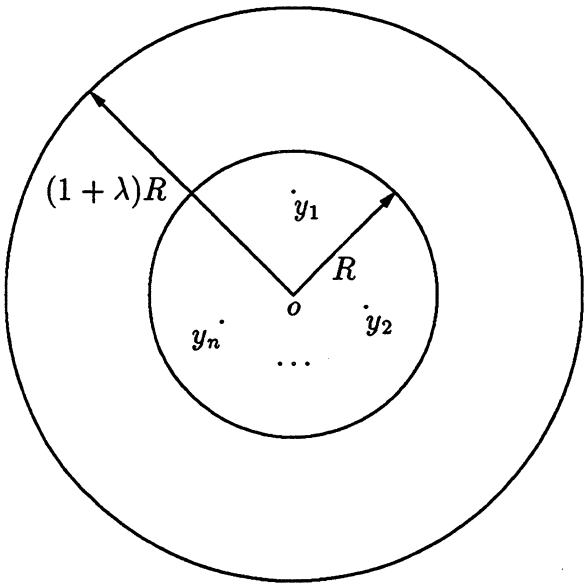

Figure 4.1: Points $\{x_i\}$ outside the circle with radius $(1+\lambda)R$

interaction matrix of the two sets $\{x_i\}$ *and* $\{y_j\}$ *has the decomposition*

$$\left(\phi_{y_j}(x_i)\right) = \begin{pmatrix} \ln x_1 & \frac{1}{x_1} & \frac{1}{x_1^2} & \cdots & \frac{1}{x_1^p} \\ \ln x_2 & \frac{1}{x_2} & \frac{1}{x_2^2} & \cdots & \frac{1}{x_2^p} \\ \vdots & \vdots & \vdots & & \vdots \\ \ln x_m & \frac{1}{x_m} & \frac{1}{x_m^2} & \cdots & \frac{1}{x_m^p} \end{pmatrix} \begin{pmatrix} 1 & 1 & \cdots & 1 \\ \frac{-y_1}{1} & \frac{-y_2}{1} & \cdots & \frac{-y_m}{1} \\ \frac{-y_1^2}{2} & \frac{-y_2^2}{2} & \cdots & \frac{-y_m^2}{2} \\ \vdots & \vdots & \vdots & \vdots \\ \frac{-y_1^p}{p} & \frac{-y_2^p}{p} & \cdots & \frac{-y_m^p}{p} \end{pmatrix} + E^p, \quad (4.11)$$

where the truncation error $E^p = \left(\varepsilon^p_{y_j}(x_i)\right)$ *is bounded by the expression*

$$\left|\varepsilon^p_{y_j}(x_i)\right| \leq (\frac{1}{\lambda})(\frac{1}{1+\lambda})^p \quad (4.12)$$

for $1 \leq i \leq m$ *and* $1 \leq j \leq n$.

Inequality (4.12) means that every element of the matrix of truncation error E^p decays exponentially as the function of p. Thus for any given accuracy, the interaction matrix of the two sets $\{x_i\}$ and $\{y_j\}$ can be decomposed into the product of two matrices of low rank ($\leq (p+1)$).

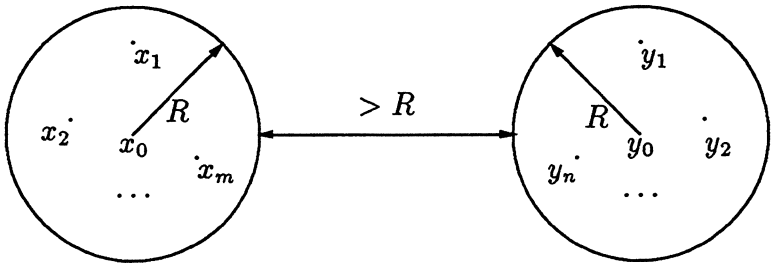

Figure 4.2: Well-separated sets in the plane

For two sets of points, $\{x_1, x_2, \cdots, x_m\} \in \mathbb{C}$ and $\{y_1, y_2, \cdots, y_n\} \in \mathbb{C}$, we say that the two sets are *well-separated* (see Figure 4.2) if there exist points $x_0, y_0 \in \mathbb{C}$, and $R > 0$ such that

$$|x_i - x_0| < R \quad \text{for } 1 \leq i \leq m,$$

$$|y_j - y_0| < R \quad \text{for } 1 \leq j \leq n,$$

$$|x_0 - y_0| > 3R.$$

Theorem 4.1 implies that with any prescribed precision, the interaction matrix of two well-separated sets can be decomposed into a product of two matrices of low rank, the rank depending only on the separation of the two sets ($\lambda > 1$), (see formula (4.12)).

4.2 Interactions in Cantor Sets

In this section, we consider electrostatic interactions within a Cantor set C^a. For any given ratio a, the interactions in the Cantor set C^a are of low rank. The interaction ranks depend only on the ratio a for generating the Cantor set.

The following lemma is obvious, and will be used in the proof of Theorem 4.2.

Lemma 4.2 *Suppose that D_1 and D_2 are two subsets of Cantor set C^a with ratio a, set A is a child box of D_1, and B is a child box of D_2 (see Figure 4.3). Then the rank*

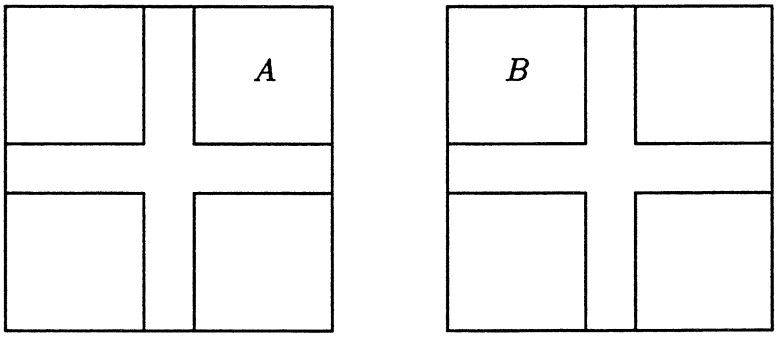

Figure 4.3: Two Subsets of C^a and Their Child Boxes

of the interaction matrix between subsets D_1 and D_2 at most four times as large as that between boxes A and B.

Theorem 4.2 *For a given real number a ($0 < a < \frac{1}{2}$), and an integer $l \geq 1$, suppose that C^a is the Cantor set associated with the ratio a, and C_l^a is the set of boxes generated at the $l-th$ level*

$$C_l^a = \{D_1, D_2, \cdots, D_{4^l}\}. \tag{4.13}$$

Then for any given precision, the rank of the interaction matrix between any two boxes D_i and D_j depends only the ratio a for generating the Cantor set C^a, and does not depend on the sizes of boxes and the numbers of points inside the boxes.

In other words, the matrix of interactions between any two boxes at any level of Cantor set C^a is of fixed rank, to any prescribed precision.

Proof: Because of the self-similarity of the Cantor set C^a, it is sufficient to estimate the rank of interactions between any two boxes of C_l^a with $l = 1$,

$$C_1^a = \{D_1, D_2, D_3, D_4\}.$$

Suppose that D_1 and D_2 are not well-separated. Then we divide each of them into four squares of the same size (see Figure 4.4). Let A be a square from the subdivision of D_1, and B be a square from the subdivision of D_2.

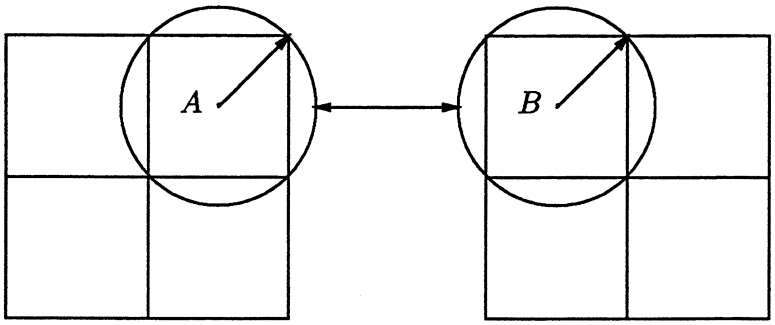

Figure 4.4: Subdivisions of Two Sets

If squares A and B are well-separated, then the rank of interaction between D_1 and D_2 is no greater than $4p$, where p is the interaction rank between A and B.

If A and B are not well-separated, then we keep dividing each region into four squares till the pieces are well-separated.

Due to Lemma 4.2 and Theorem 4.1, the rank of the interaction matrix between any two boxes at any level of the Cantor set is bounded by

$$p \cdot 4^k \qquad \text{with} \qquad k = \left| \frac{\ln(1-2a)/(\sqrt{2}-1)}{\ln a} \right|, \tag{4.14}$$

where p is the rank of the interaction matrix between two well-separated boxes. ■

Remark 4.2 *Clearly, the estimate (4.14) is an extremely pessimistic one. In the following chapter, we obtain much sharper numerical estimates (see section 5.3).*

Chapter 5

Scattering Theory for the Laplace Equation

In this chapter, we borrow terminology from the standard scattering theory of wave equations for the design of fast algorithms, and refer to the result as scattering theory for the Laplace equation.

To develop the scattering theory for the Laplace equation, we first introduce the concept of scattering matrix, and then present the merging scheme for generating scattering matrices recursively.

Throughout this section, Γ will denote a Jordan curve, parameterized by its length $\gamma : [0, L] \rightarrow R^2$. The region bounded by Γ will be denoted by Ω, and D will denote a compact subset of Ω. In addition, G: $\Omega \times \Omega \rightarrow R^1$ will denote the Green's function for domain Ω, and $N : [0, L] \rightarrow R^2$ will denote the interior normal to Γ. For a compact set $E \subset R^2$, $\mathcal{M}(E)$ will denote the set of all non-negative Borel measures on E.

5.1 Scattering Matrices

Any function $\Phi : \overline{\Omega} \rightarrow R$ harmonic inside Ω and continuous on $\overline{\Omega}$ will be referred to as **incoming potential.** As is well-known, for any continuous function $\varphi : \Gamma \rightarrow R$,

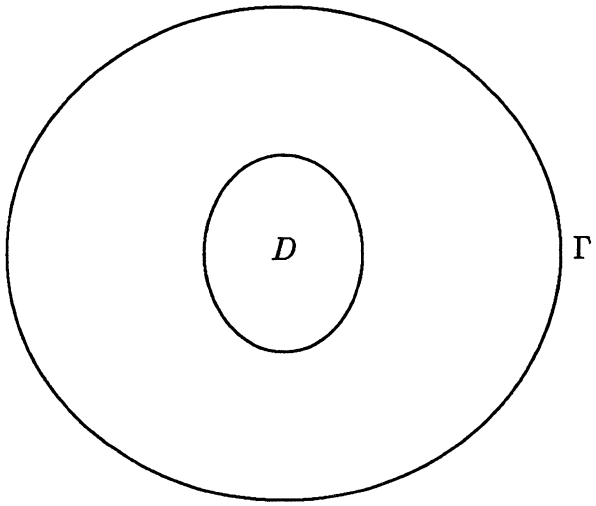

Figure 5.1: Compact set D in domain Ω with boundary Γ

there exists a unique function $\Phi : \overline{\Omega} \to R$ harmonic on Ω, and continuous on $\overline{\Omega}$ such that $\Phi|_\Gamma = \varphi$. Therefore, we will abuse the notation by referring to the function $\varphi : \Gamma \to R$ as the incoming potential.

Suppose that $q \in L^2(\Omega)$ and σ is a Borel measure over D. Given a function $K \in L^2(R^2 \times R^2)$, the function

$$\Psi(x) = \int_D K(x,t)q(t)d\sigma(t) \quad \text{for } x \in R^2 \backslash D \tag{5.1}$$

will be referred to as **outgoing potential.** Similarly, we will call its restriction $\psi = \Psi|_\Gamma$ onto Γ an outgoing potential. Outside the domain $\overline{\Omega}$, function Ψ will also be referred to as **scattering potential.**

Remark 5.1 *Particularly, we are interested in the case when* $K(x,t) = \ln||x-t||$, *and* $q(t)$ *is the characteristic function of* D. *Then the outgoing potential*

$$\Psi(x) = \int_D \ln||x-t||d\sigma(t) \tag{5.2}$$

is a function harmonic in $R^2 \backslash D$, *and satisfying the far field condition (2.8).*

We define three operators

$$L : L^2(\Gamma) \to L^2(D),$$

$$P : \mathcal{M}(D) \to L^2(R^2 \backslash D),$$

$$S : \mathcal{M}(D) \to L^2(\Gamma),$$

via the formulae

$$L(\varphi)(x) = \frac{1}{2\pi} \int_0^L \varphi(\gamma(t)) \cdot \frac{\partial}{\partial N_t} G(x, \gamma(t)) \cdot dt, \tag{5.3}$$

$$P(\sigma)(x) = \int_D K(x,t) q(t) d\sigma(t) \qquad \text{for } x \in R^2 \backslash D, \tag{5.4}$$

$$S(\sigma)(x) = \int_D K(x,t) q(t) d\sigma(t) \qquad \text{for } x \in \Gamma. \tag{5.5}$$

We will be considering equations of the form

$$P(\sigma) = f, \tag{5.6}$$

with $f \in L^2(D)$. A special case of equation (5.6) is the integral equation (2.9) defined in section 2.2, with D a Cantor set, $K(x,t) = \ln ||x - t||$, and $q(t)$ the characteristic function of D.

Definition 5.1 *The operator $\alpha : L^2(\Gamma) \to L^2(\Gamma)$ defined by the expression*

$$\alpha = S \cdot P^{-1} \cdot L \tag{5.7}$$

will be referred to as **scattering matrix.**

Remark 5.2 *Given an incoming potential φ on the boundary Γ, the operation of α on φ can be viewed as consisting of three steps:*

1. *The operator L constructs a function $f = L\varphi : \overline{\Omega} \to R$ harmonic over the compact set D, and such that $(L\varphi)|_\Gamma = \varphi$.*

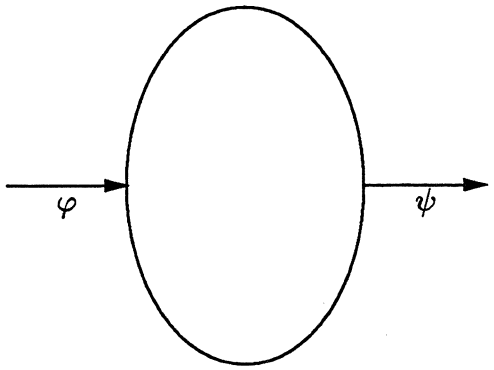

Figure 5.2: Scattering matrix α: $\varphi \to \psi$

2. *The operator P^{-1} constructs the solution $\sigma = P^{-1}f$ of equation (5.6) from the harmonic function $f = L\varphi$.*

   The charge distribution σ will be referred to as **induced charge distribution.**

3. *The operator S defined by (5.5) constructs an outgoing potential $\psi = S\sigma$ on Γ from the induced charge distribution σ.*

   The outgoing potential ψ will be referred to as **induced outgoing potential.**

Thus, the scattering matrix α maps an incoming potential φ to the induced outgoing potential ψ

$$\psi = \alpha\varphi. \tag{5.8}$$

The following theorem, while interesting in itself, is not closely related to the purpose of this thesis since its proof is quite involved. We refer the reader to [15] and [55], where it can be found in a somewhat different form.

Theorem 5.1 (Compactness of Scattering Matrix α) *Suppose that $K(x,t) = \ln||x-t||$, and $q(t)$ is the characteristic function of D. If $D \cap \Gamma = \emptyset$, then the scattering matrix α in (5.7) is a compact operator.*

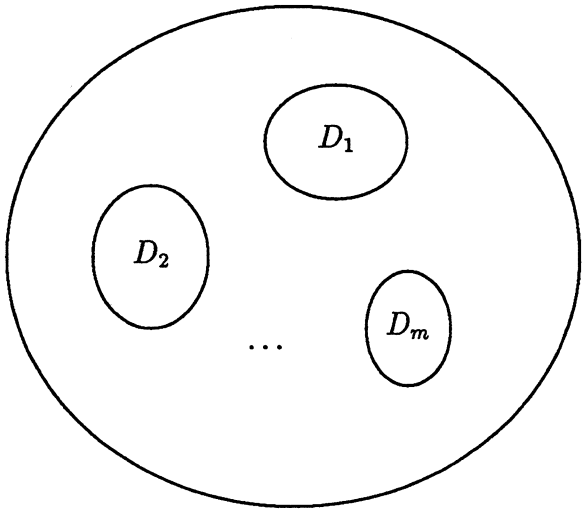

Figure 5.3: Disjoint compact sets $\{D_i\}$ in domain Ω

In other words, if D is strictly inside domain Ω (bounded by Γ), then the discretization of Γ results in the finite dimensional approximation to the scattering matrix, to any prescribed precision.

5.2 Recursive Generation of Scattering Matrices

We will consider a case when a compact subset D of domain Ω is the union of mutually disjoint compact sets $\{D_i\}$ (see Figure 5.3).

It turns out that the scattering matrix of D can be obtained by merging the scattering matrices of $\{D_i\}$. We begin with introducing the requisite notation. Then we present the merging scheme for the recursive generation of scattering matrices.

5.2.1 Notation

Suppose that $\Delta = \{\Gamma_1, \Gamma_2, \cdots, \Gamma_m\} \subset \Omega$ is a set of closed Jordan curves. Each $\Gamma_i \in \Delta$ is parameterized by its length $\gamma_i : [0, L_i] \to R^2$, and $\Omega_i \subset \Omega$ is the region bounded by Γ_i. Suppose further that for $1 \leq i \leq m$, D_i is a compact subset of Ω_i, function G_i:

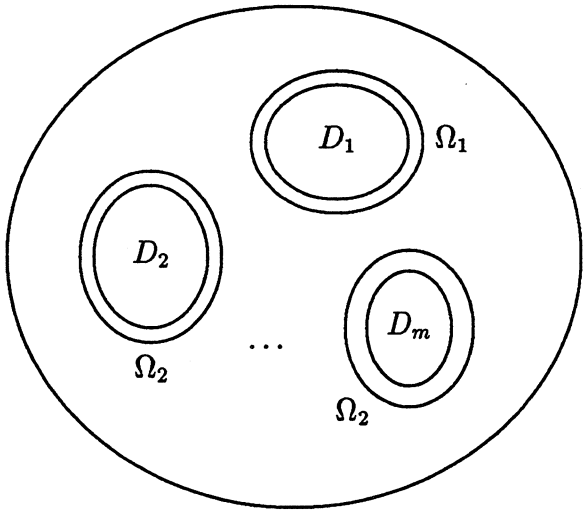

Figure 5.4: $D_i \subset \Omega_i$ for $1 \leq i \leq m$

$\Omega_i \times \Omega_i \to R^1$ is the Green's function for domain Ω_i, and function $N_i : [0, L] \to R^2$ is the interior normal to Γ_i.

Assuming the domains $\{\Omega_i\}$ to be mutually disjoint, we will consider the compact subset D of domain Ω defined by the formula

$$D = \bigcup_{i=1}^{m} D_i.$$

In addition to operators L, P, and S defined by (5.3), (5.4), and (5.5) in the preceding section, we will require the operators for $1 \leq i \leq m$

$$L_{ii} : L^2(\Gamma_i) \to L^2(\Omega_i)$$

$$P_i : \mathcal{M}(D_i) \to L^2(R^2 \backslash D_i)$$

$$S_{ii} : \mathcal{M}(D_i) \to L^2(\Gamma_i)$$

defined by formulae

$$L_{ii}(\varphi)(x) = \frac{1}{2\pi} \int_0^{L_i} \varphi(\gamma_i(t)) \cdot \frac{\partial}{\partial N_i} G_i(x, \gamma_i(t)) \cdot dt \tag{5.9}$$

$$P_i(\sigma)(x) = \int_{D_i} K(x,t)q(t)d\sigma(t) \qquad \text{for } x \in R^2 \backslash D \tag{5.10}$$

$$S_{ii}(\sigma)(x) = \int_{D_i} K(x,t)q(t)d\sigma(t) \qquad \text{for } x \in \Gamma_i. \tag{5.11}$$

We will consider equations of the form

$$P_i(\sigma) = f \tag{5.12}$$

with $f \in L^2(D_i)$, and $1 \leq i \leq m$.

Definition 5.2 *A function $\varphi_i \in L^2(\Gamma_i)$ will be called* **total incoming potential** *if for any $x \in D_i$,*

$$P_i(\sigma|_{D_i})(x) = L_{ii}(\varphi_i)(x), \tag{5.13}$$

where operators P_i and L_{ii} are defined by (5.10) and (5.9) respectively, and $\sigma|_{D_i}$ is the restriction of the charge distribution σ (defined by (5.4)) to the compact subset $D_i \subset D$.

Suppose that for any i $(1 \leq i \leq m)$, function φ_i is the total incoming potential on Γ_i, function ψ_i is the outgoing potential induced by φ_i, and operator α_i is the scattering matrix for the domain D_i. Then

$$\alpha_i = S_{ii}P_i^{-1}L_{ii}, \tag{5.14}$$

$$\psi_i = \alpha_i \cdot \varphi_i, \tag{5.15}$$

(see (5.9), (5.10), (5.11), (5.7), and (5.8)).

We will also require operators

$$L_i : L^2(\Gamma) \to L^2(\Gamma_i),$$

$$S_i : L^2(\Gamma_i) \to L^2(\Gamma),$$

$$L_{ji} : L^2(\Gamma_i) \to L^2(\Gamma_j), \quad i \neq j,$$

defined for $1 \leq i, j \leq m$ via formulae

$$L_i(\varphi)(x) = \frac{1}{2\pi}\int_0^L \varphi(\gamma(t)) \cdot \frac{\partial}{\partial N_t} G(x, \gamma(t)) \cdot dt \qquad \text{for } x \in \Gamma_i, \tag{5.16}$$

$$S_i\psi_i = \int_{D_i} K(x,t)q(t)d\sigma(t) \qquad \text{for } x \in \Gamma, \tag{5.17}$$

$$L_{ji}\psi_i = \int_{D_i} K(x,t)q(t)d\sigma(t) \qquad \text{for } x \in \Gamma_j. \tag{5.18}$$

In other words, the operator S_i converts the outgoing potential ψ_i on Γ_i into the scattering potential on Γ, and the operator L_{ji} converts the outgoing potential ψ_i on Γ_i into the scattering potential on Γ_j.

Definition 5.3 *The operator*

$$S_p : L^2(\Gamma) \to \begin{pmatrix} L^2(\Gamma_1) \\ L^2(\Gamma_2) \\ \vdots \\ L^2(\Gamma_m) \end{pmatrix}$$

defined by the formula

$$S_p = \begin{pmatrix} I & -L_{12}\alpha_2 & \cdots & -L_{1m}\alpha_m \\ -L_{21}\alpha_1 & I & \cdots & -L_{2m}\alpha_m \\ \vdots & \vdots & \cdots & \vdots \\ -L_{m1}\alpha_1 & -L_{m2}\alpha_2 & \cdots & I \end{pmatrix}^{-1} \begin{pmatrix} L_1 \\ L_2 \\ \vdots \\ L_m \end{pmatrix} \tag{5.19}$$

will be referred to as **splitting matrix**, *provided the inverse in (5.19) exists.*

5.2.2 Merging Scheme for Scattering Matrices

Lemma 5.1 is used in the construction of the merging scheme for scattering matrices, and Theorem 5.2 gives the full description of the scheme.

Lemma 5.1 *Suppose that φ is an incoming potential on the boundary Γ, and φ_i is the total incoming potential on Γ_i in the sense of (5.13). If the inverse in (5.19) exists, then*

$$\begin{pmatrix} \varphi_1 \\ \varphi_2 \\ \vdots \\ \varphi_m \end{pmatrix} = S_p \cdot \varphi. \tag{5.20}$$

In other words, the splitting matrix maps the incoming potential φ on Γ to the total incoming potentials $\{\varphi_i\}$ on boundaries $\{\Gamma_i\}$.

Proof: For any i $(1 \leq i \leq m)$, the total incoming potential φ_i on the boundary Γ_i equals to the sum of the potential from Γ and the scattering potentials from $\{\Gamma_j\}$ with $j \neq i$ and $1 \leq j \leq m$. That is,

$$\varphi_i = L_i\varphi + \sum_{j \neq i} L_{ij}\psi_j. \tag{5.21}$$

Combining (5.15) with (5.21), we have

$$\varphi_i = L_i\varphi + \sum_{j \neq i} L_{ij}\alpha_j\varphi_j. \tag{5.22}$$

Viewing the above equations as a $m \times m$ linear system, we obtain (5.20). ■

Theorem 5.2 (Recursive Generation of Scattering Matrices) *Given scattering matrices $\{\alpha_i\}$ for domains $\{D_i\}$, the scattering matrix α of domain D is given by the formula*

$$\alpha = \begin{pmatrix} S_1\alpha_1 & S_2\alpha_2 & \cdots & S_m\alpha_m \end{pmatrix} S_p, \tag{5.23}$$

where operators $\{S_i\}$ are defined by (5.17), and the splitting matrix S_p is defined by (5.19).

Proof: Suppose that φ is an incoming potential on Γ, and σ is the charge distribution induced by φ. Then by definition (see equation (5.1)), the induced outgoing potential

ψ assumes the form

$$\begin{aligned} \psi(x) &= \int_D K(x,t) \cdot q(t) \cdot d\sigma(t) \\ &= \sum_{i=1}^{m} \int_{D_i} K(x,t) \cdot q(t) \cdot d\sigma(t) \end{aligned} \tag{5.24}$$

for any $x \in \Gamma$.

By definition of the operator S_i in (5.17),

$$S_i \psi_i = \int_{D_i} K(x,t) q(t) dt, \tag{5.25}$$

so that equation (5.24) assumes the form

$$\psi(x) = \sum (S_i \cdot \psi_i)(x). \tag{5.26}$$

Therefore,

$$\begin{aligned} \psi &= \sum S_i \cdot \psi_i = \sum S_i \cdot \alpha_i \cdot \varphi_i \\ &= \begin{pmatrix} S_1\alpha_1 & S_2\alpha_2 & \cdots & S_m\alpha_m \end{pmatrix} \begin{pmatrix} \varphi_1 \\ \varphi_2 \\ \vdots \\ \varphi_m \end{pmatrix}. \end{aligned} \tag{5.27}$$

Now, the conclusion of the theorem follows from the combination of (5.27), (5.7), and Lemma 5.1. ■

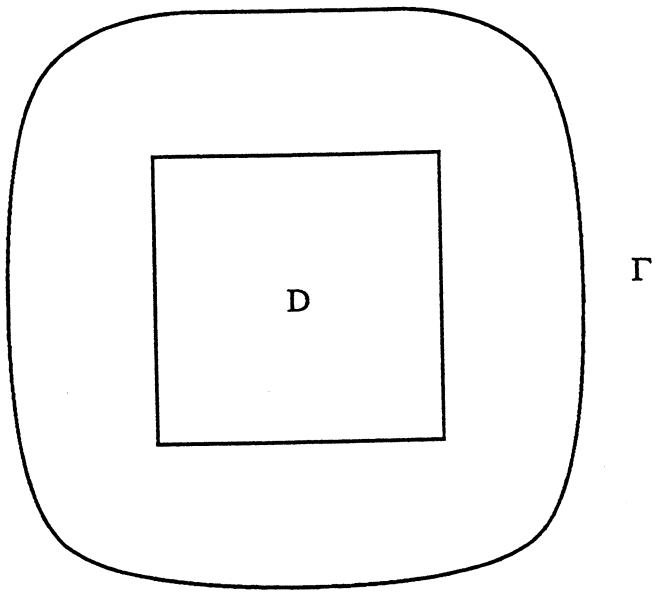

Figure 5.5: A subset D of Cantor set C^a in domain Ω

5.3 Scattering Matrices in Cantor Sets

Suppose that D is a compact subset of Cantor set C^a, and the set D is enclosed in a domain Ω with its boundary denoted by Γ (see Figure 5.5). The boundary Γ will be referred to as frame boundary.

To specifically deal with the problem defined in section 2.2, we consider scattering matrices in Cantor sets, with $K(x,t) = \ln||x-t||$ and $q(t)$ as the characteristic function of D. Then an incoming potential Φ is harmonic in Ω, and an outgoing potential Ψ is harmonic in $R^2\backslash D$, and satisfying the far-field condition (2.8) (see Remark 5.1).

The operators $P : L^2(D) \to L^2(R^2\backslash D)$ defined by formula (5.4), and $S : L^2(D) \to L^2(\Gamma)$ defined by formula (5.5) assume the form

$$P(\sigma)(x) = \int_D \ln||x-t||d\sigma(t), \tag{5.28}$$

$$S(\sigma)(x) = \int_D \ln||x-t||d\sigma(t). \tag{5.29}$$

In this section, we construct an analytical apparatus for representing scattering matrices corresponding to subsets of Cantor sets. First, we discuss the representations of incoming and outgoing potentials in terms of single and double layer distributions.

5.3.1 Representation of Potentials

Lemma 5.2 below is an obvious statement about the representations of incoming and outgoing potentials in terms of the solutions of classical boundary value problems for the Laplace equation, and Lemma 5.3 is a statement about the representations of incoming and outgoing potentials in terms of the solutions of integral equations in the potential theory (see section 3.1). Theorem 5.3 is an immediate consequence of Lemma 5.3, and Theorem 5.4 follows immediately from Lemma 3.1 and Theorem 5.3.

Lemma 5.2 *Suppose that φ is an incoming potential on the boundary Γ, and ψ is an outgoing potential on Γ. Then the incoming and outgoing potentials Φ and Ψ are respectively the solutions of the following two boundary value problems.*

(AA) Interior Dirichlet problem (Incoming Potential)

$$\begin{aligned} \Delta\Phi(x) &= 0 && \text{for} \quad x \in \Omega \\ \Phi(x) &= \varphi(\gamma^{-1}(x)) && \text{for} \quad x \in \Gamma \end{aligned} \tag{5.30}$$

(BB) Exterior Neumann problem(Outgoing Potential)

$$\begin{aligned} \Delta\Psi(x) &= 0 && \text{for} \quad x \in R^2 \backslash \Omega \\ \tfrac{\partial}{\partial N}\Psi(x) &= \psi(\gamma^{-1}(x)) && \text{for} \quad x \in \Gamma \end{aligned} \tag{5.31}$$

with Ψ satisfying the far-field condition (2.8).

Lemma 5.3 *Suppose that φ is an incoming potential on the boundary Γ, and ψ is an outgoing potential on Γ. Suppose further that a dipole distribution μ_d and a charge distribution μ_s are respectively the solutions of the two integral equations,*

$$\pi\mu_d(x) + \int_0^L \frac{\partial}{\partial N(t)} \log||\gamma(x) - \gamma(t)||\mu_d(t)dt = \varphi(x) \tag{5.32}$$

$$-\pi\mu_s(x)+\frac{\partial}{\partial N(x)}\int_0^L \log||\gamma(x)-\gamma(t)||\mu_s(t)dt=\psi(x). \tag{5.33}$$

Then the incoming and outgoing potentials can be represented by the formulae

$$\Phi(x)=\int_0^L \frac{\partial}{\partial N(t)}\log||\gamma(x)-\gamma(t)||\mu_d(t)dt, \tag{5.34}$$

$$\Psi(x)=\int_0^L \log||\gamma(x)-\gamma(t)||\mu_s(t)dt. \tag{5.35}$$

To formulate the above theorem in the operator notation, we define four operators

$$Q_d: L^2(\Gamma)\to L^2(\Omega),$$

$$Q_s: L^2(\Gamma)\to L^2(R^2\backslash\Omega),$$

$$P_d: L^2(\Gamma)\to L^2(\Gamma),$$

$$P_s: L^2(\Gamma)\to L^2(\Gamma),$$

via formulae

$$Q_d(\mu_d)(x)=\int_0^L \frac{\partial}{\partial N(t)}\log||\gamma(x)-\gamma(t)||\mu_d(t)dt, \tag{5.36}$$

$$Q_s(\mu_s)(x)=\int_0^L \log||\gamma(x)-\gamma(t)||\mu_s(t)dt, \tag{5.37}$$

$$P_d(\mu_d)(x)=\pi\mu_d(x)+\int_0^L \frac{\partial}{\partial N(t)}\log||\gamma(x)-\gamma(t)||\mu_d(t)dt, \tag{5.38}$$

$$P_s(\mu_s)(x)=-\pi\mu_s(x)+\frac{\partial}{\partial N(x)}\int_0^L \log||\gamma(x)-\gamma(t)||\mu_s(t)dt. \tag{5.39}$$

Theorem 5.3 *Suppose that φ is an incoming potential on the boundary Γ, and ψ is an outgoing potential on Γ. Then the incoming and outgoing potentials can be represented via the formulae*

$$\Phi=Q_dP_d^{-1}\varphi, \tag{5.40}$$

$$\Psi=Q_sP_s^{-1}\psi, \tag{5.41}$$

where operators Q_s, Q_d, P_s and P_d are defined by (5.37), (5.36), (5.39), and (5.38) respectively.

Theorem 5.4 *Suppose that $L : L^2(\Gamma) \to L^2(D)$ is the operator defined by the formula (5.3). Then*

$$L\varphi = (Q_d P_d^{-1}\varphi)|_D, \tag{5.42}$$

with the operators Q_d and P_d defined by the formulae (5.36) and (5.38) respectively.

Remark 5.4 *Under certain circumstances, we will be generating scattering matrices directly by using their definition (see (5.7))*

$$\alpha = SP^{-1}L, \tag{5.43}$$

where operators P, S, and L are defined by formulae (5.28), (5.29), and (5.42) respectively.

5.3.2 Recursive Generation Of Scattering Matrices

Suppose that $\{D_1, D_2, D_3, D_4\} \subset C^a$ are four subsets (boxes) resulting from the subdivision of a bigger subset (box), and the set D is the union the four subsets $\{D_i\}$

$$D = \bigcup_{i=1}^{4} D_i. \tag{5.44}$$

Suppose further that D is enclosed in s square Ω with its boundary denoted by Γ. The square Ω will be referred to as frame domain (box) while Γ is referred to as frame boundary.

Suppose that for any integer i $(1 \leq i \leq m)$, the set D_i is enclosed in a square Ω_i with its boundary denoted by Γ_i (see Figure 5.6). Within the tree structure of the Cantor set C^a (see section 2.1), we will refer the frame boxes of neighbor boxes as *frame neighbor boxes*, and the frame box of a parent box as *parent frame box.*

In this section, we obtain the scattering matrix α for D from scattering matrices $\{\alpha_1, \alpha_2, \alpha_3, \alpha_4\}$ for domains $\{D_1, D_2, D_3, D_4\}$. First, we need the representations of operators

$$L_i : L^2(\Gamma) \to L^2(\Gamma_i),$$

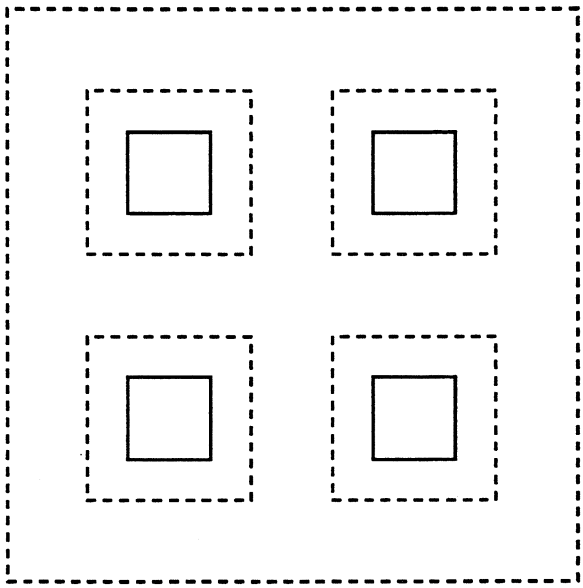

Figure 5.6: Four Subsets of C^a and Their Frame Boxes

$$S_i : L^2(\Gamma_i) \to L^2(\Gamma),$$

$$L_{ji} : L^2(\Gamma_i) \to L^2(\Gamma_j),$$

defined by formulae (5.16), (5.17), and (5.18) respectively.

Theorems 5.5 and 5.6 below follow from Theorem 5.3 immediately, Lemma 5.4 is the immediate consequence of Lemma 5.1, and Theorem 5.7 is the consequence of Theorem 5.2 and Lemma 5.4. Theorems 5.5 and 5.6 describe representations of the operators L_i, S_i, and L_{ij} defined by formulae (5.16), (5.17), and (5.18). And Theorem 5.7 describes the merging scheme for the recursive generation of scattering matrices for subsets of Cantor sets.

Theorem 5.5 *Suppose that $L_i : L^2(\Gamma) \to L^2(\Gamma_i)$ is the operator defined via formula (5.16). Then*

$$L_i\varphi = (Q_d P_d^{-1}\varphi)|_\Gamma, \tag{5.45}$$

with operators Q_d and P_d defined by formulae (5.36)and (5.38) respectively.

Similar to operators Q_s defined by formula (5.37) and P_s defined by formula (5.39) for domain Ω, we define operators on domain Ω_i for $1 \leq i \leq 4$,

$$Q_{s,i} : L^2(\Gamma_i) \to L^2(R^2 \backslash \Omega_i),$$

$$P_{s,i} : L^2(\Gamma_i) \to L^2(\Gamma_i),$$

by formulae

$$Q_{s,i}(\sigma_s)(x) = \int_0^{L_i} \log ||\gamma_i(x) - \gamma_i(t)|| \sigma_s(t) dt, \tag{5.46}$$

$$P_{s,i}(\sigma_s)(x) = -\pi \sigma_s(x) + \frac{\partial}{\partial N_i(x)} \int_0^{L_i} \log ||\gamma_i(x) - \gamma_i(t)|| \sigma_s(t) dt. \tag{5.47}$$

Theorem 5.6 *Suppose that operator*

$$S_i : L^2(\Gamma_i) \to L^2(\Gamma),$$

is defined via formula (5.17), and operator

$$L_{ji} : L^2(\Gamma_i) \to L^2(\Gamma_j) \qquad \text{for } i \neq j,$$

is defined via formula (5.18). Then

$$S_i \psi = (Q_{s,i} P_{s,i}^{-1} \psi)|_\Gamma, \tag{5.48}$$

$$L_{ji} \psi = (Q_{s,i} P_{s,i}^{-1} \psi)|_{\Gamma_j}, \tag{5.49}$$

with operators $Q_{s,i}$ and $P_{s,i}$ defined by formulae (5.46) and (5.47) respectively.

Remark 5.4 *The splittering matrix*

$$S_p : L^2(\Gamma) \to \begin{pmatrix} L^2(\Gamma_1) \\ L^2(\Gamma_2) \\ L^2(\Gamma_3) \\ L^2(\Gamma_4) \end{pmatrix}$$

is given by the expression (see formula (5.19))

$$S_p = \begin{pmatrix} I & -L_{12}\alpha_2 & -L_{13}\alpha_3 & -L_{14}\alpha_4 \\ -L_{21}\alpha_1 & I & -L_{23}\alpha_3 & -L_{24}\alpha_4 \\ -L_{31}\alpha_1 & -L_{32}\alpha_2 & I & -L_{24}\alpha_4 \\ -L_{41}\alpha_1 & -L_{42}\alpha_2 & -L_{43}\alpha_3 & I \end{pmatrix}^{-1} \begin{pmatrix} L_1 \\ L_2 \\ L_3 \\ L_4 \end{pmatrix}, \tag{5.50}$$

with L_i defined by (5.45) for $1 \leq i \leq 4$, and L_{ij} defined by (5.49) for $1 \leq i, j \leq 4$.

Lemma 5.4 *Suppose that φ is an incoming potential on the boundary Γ, and for $1 \leq i \leq 4$, φ_i is the total incoming potential on Γ_i in the sense of (5.13). Then*

$$\begin{pmatrix} \varphi_1 \\ \varphi_2 \\ \varphi_3 \\ \varphi_4 \end{pmatrix} = S_p \cdot \varphi, \tag{5.51}$$

with the splitting matrix S_p defined by formula (5.50).

In other words, the splitting matrix maps the incoming potential φ on Γ to the total incoming potentials $\{\varphi_i\}$ on boundaries $\{\Gamma_i\}$.

Theorem 5.7 *Suppose that for $1 \leq i \leq 4$, the scattering matrix for the compact set D_i is denoted by α_i. Then the scattering matrix α for the set $D = \bigcup_{i=1}^{4} D_i$ is given by the merging formula*

$$\alpha = \begin{pmatrix} S_1\alpha_1 & S_2\alpha_2 & S_3\alpha_3 & S_4\alpha_4 \end{pmatrix} S_p, \tag{5.52}$$

with operator S_i defined by formula (5.48) for $1 \leq i \leq 4$, and the splitting matrix S_p defined by formula (5.50).

Remark 5.5 *Due to the self-similarity in Cantor sets (see section 2.1), we only need to compute one scattering matrix per level.*

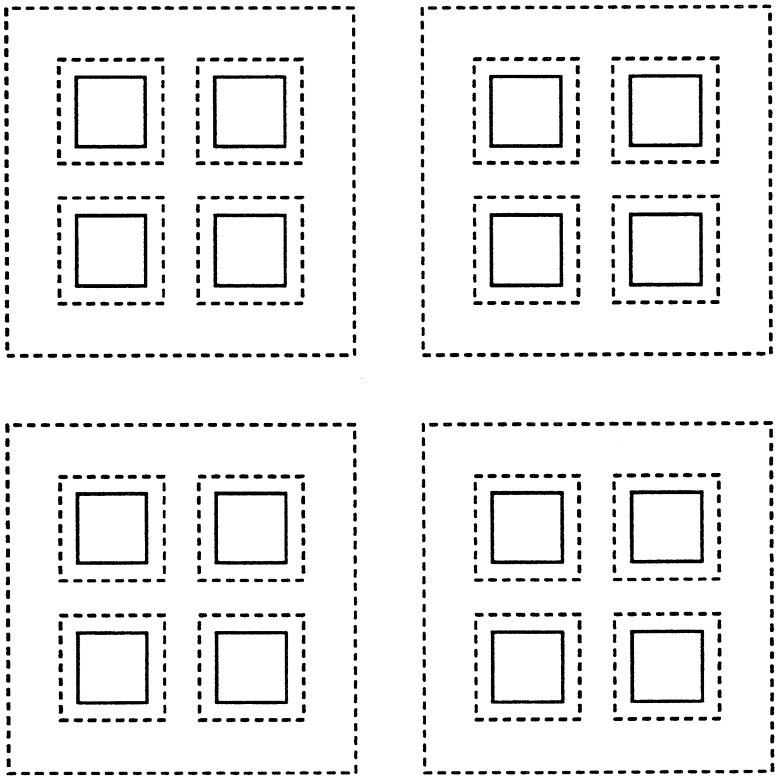

Figure 5.7: Frame Boxes for Cantor Set C^a

5.3.3 Discretization of Scattering Matrices

From the preceding sections, it is clear that the construction of scattering matrices for subsets of Cantor sets, either directly or recursively, depends on the choice of frame boundaries (or frame boxes) (see Remark 5.4 and Theorem 5.7). For a Cantor set C^a, we recursively generate frame boxes for subsets of C^a such that frame boxes at the same level are mutually disjoint, and the distance between a box and its frame box equals to the distance between two neighbor frame boxes (see Figure 5.7).

With the above choice of frame boxes, we first represent incoming and outgoing potentials Φ and Ψ numerically in the forms described in Theorem 5.3, in order to discretize scattering matrices for subsets of Cantor sets.

Lemma 5.5 below introduces a set of orthogonal polynomials, and Lemmas 5.6

and 5.59 describe the two-dimensional integrations involved in the application of the Galerkin method to the numerical representation of incoming and outgoing potentials (see sections 3.2 and 5.3.1).

Lemma 5.5 *Suppose that* $\{P_1(x), P_2(x), \cdots, P_n(x), \cdots\}$ *is a set of polynomials defined by the formulae*

$$P_n(x) = \frac{n!}{(2n)!}\frac{d^n}{dx^n}(x^2-1)^n, \qquad n = 0, 1, 2, \cdots. \tag{5.53}$$

Then

$$\int_{-1}^{-1} P_i(x)P_j(x)dx = 0 \qquad \text{for } i \neq j. \tag{5.54}$$

The orthogonal polynomials defined above are the well-known **Legendre polynomials**. The roots of $P_n(x)$ will be referred to as the Legendre nodes. We will use the Legendre polynomials in the Galerkin method as the basis functions to represent incoming and outgoing potentials numerically in terms of the representations described in Theorem 5.3.

Lemma 5.6 *Suppose that* Ω *is a square of size two with its boundary denoted by* Γ, *and* $\{P_1(x), P_2(x), \cdots, P_n(x), \cdots\}$ *are the Legendre orthogonal polynomials defined in Lemma 5.5. Suppose further that* μ *is either the solution of equation (5.32) or of equation (5.33), and the solution* μ *is approximated by the truncated expansion on each side of the square* Ω*:*

$$\mu_n(x) = \sum_{i=0}^{n} \xi_i P_i(x), \tag{5.55}$$

for each of the two horizontal sides of Ω, *and*

$$\mu_n(y) = \sum_{i=0}^{n} \eta_i P_i(y), \tag{5.56}$$

for each of the two vertical sides of Ω. *Then there are only two types of integrations involved in the matrices of the type defined by formula (3.17) in the Galerkin method described in section 3.2. The two integrations are of the form*

$$I_{ij} = \int_{-1}^{1}\int_{-1}^{1} \frac{(y+1)}{(x+1)^2+(y+1)^2} P_i(x)P_j(x)dxdy, \tag{5.57}$$

for any two adjacent sides of domain Ω, and

$$J_{ij} = \int_{-1}^{1}\int_{-1}^{1} \frac{2}{(x-y)^2+4} P_i(x)P_j(x)dxdy, \tag{5.58}$$

for non-adjacent sides of domain Ω, where $1 \leq i,j \leq n$.

The following lemma is obtained immediately by writing down the integral I_{ij} (defined by (5.57)) in polar coordinates.

Lemma 5.7 *Suppose that for $1 \leq i,j \leq n$, integration I_{ij} is defined by (5.57). Then*

$$I_{ij} = \{\int_0^{\frac{\pi}{4}}\int_0^{\frac{2}{\cos\theta}} + \int_{\frac{\pi}{4}}^{\frac{\pi}{2}}\int_0^{\frac{2}{\sin\theta}}\} P_i(r\cos\theta - 1)P_j(r\sin\theta - 1)\sin\theta dr d\theta. \tag{5.59}$$

Remark 5.6 *Integrations I_{ij} defined by formula (5.59) and J_{ij} defined by formula (5.58) for $1 \leq i,j \leq n$, are now integrals of smooth functions. They can be computed by the Gaussian quadrature rule based on Legendre nodes (see, for example, [50]). Thus, operators P_d and P_s can be represented numerically by the formulae (5.38) and (5.39) respectively.*

On the other hand, with the approximated solution μ_n (defined by (5.55) and (5.56)) to μ the solution of either equation (5.32) or (5.33), operators Q_d and Q_s defined by formulae (5.36) and (5.37) can be represented numerically by using the Gaussian quadrature rule.

Therefore, incoming and outgoing potentials Φ and Ψ are represented numerically by formulae (5.40) and (5.41) respectively.

Based on the above choice of frame boxes, Tables 5.1 and 5.2 list the number of Legendre nodes needed on frame boundaries for the representation of incoming and outgoing potentials to single and double precision respectively.

$\epsilon = 10^{-7}$ (Absolute Error)

Ratio a	0.1	0.2	0.3	0.35	0.4	0.45
Number of Nodes Per Side	12	18	30	46	66	100

Table 5.1: Number of Legendre Nodes for Single Precision

$\epsilon = 10^{-14}$ (Absolute Error)

Ratio a	0.1	0.2	0.3	0.35	0.4	0.45
Number of Nodes Per Side	30	44	60	80	120	200

Table 5.2: Number of Legendre Nodes for Double Precision

Remark 5.7 *Two observations can be easily made from the above two tables.*

1. *The number of Legendre nodes needed to obtain double precision is only twice the number of nodes needed for single precision.*

2. *The number of nodes needed increases rapidly with the increase in ratio a.*

With the frame boundaries described above, we are ready to discretize scattering matrices for subsets of Cantor sets.

Suppose the the set of points $\{z_1, z_2, \cdots, z_m\}$ is the approximation to the compact set $D \subset \Omega$, and the set of points $\{x_1, x_2, \cdots, x_p\}$ are the Legendre nodes on the boundary Γ.

The operator P defined by formula (5.28) is discretized in a manner similar to that of the integral equation (2.9). In other words, the discretization of P is a matrix $\tilde{P}$ defined by the formulae

$$(\tilde{P})_{ij} = \ln ||z_i - z_j|| \quad \text{for } i \neq j \quad \text{and } 1 \leq i, j \leq m, \tag{5.60}$$

$$(\tilde{P})_{ii} = l \cdot \log a + \delta \quad \text{for } 1 \leq i \leq m, \tag{5.61}$$

where δ is a contant (see (2.11)).

Similarly, the operator S defined by (5.29) is discretized as a matrix $\tilde{S}$ defined by the formulae

$$(\tilde{S})_{ij} = \ln ||x_i - z_j|| \quad \text{for } 1 \leq i \leq p \quad \text{and } 1 \leq j \leq m. \tag{5.62}$$

The operator Q_d defined by (5.36) and the operator $Q_{s,i}$ defined by (5.46), are discretized by the Gaussian quadrature rule based on Legendre nodes. The operator P_d defined by (5.38) and the operator $P_{s,i}$ defined by (5.47) are discretized by the Galerkin method described in section 3.2.

Remark 5.8 *Given a discretization of operators P, S, P_d, Q_d, $Q_{s,i}$ and $P_{s,i}$ (defined by the formulae (5.28), (5.29), (5.38), (5.36), (5.46) and (5.47) respectively), all the other operators L, L_i, S_i, L_{ij} and S_p for $1 \leq i, j \leq 4$, are represented numerically by the formulae (5.42), (5.45) , (5.48), (5.49) and (5.50). Thus, scattering matrices can be computed either directly by using formula (5.43), or recursively by using the merging scheme described in Theorem 5.2.*

Chapter 6

The Fast Direct Algorithm

In this chapter, we describe a direct algorithm for the rapid solution of the Laplace equation on regions with fractal boundaries. The algorithm exploits the fact that for any given ratio a, interactions at any level in the Cantor set C^a are of low rank (the ranks depend only the constant ratio a for generating the Cantor set, and do not depend on the sizes of boxes and number of points inside). The low rank of interactions is reflected in the coefficient matrix in equation (2.10) as the low-rank of its off-diagonal submatrices (see Figure 6.1). Thus, we can recursively compress these matrices of low rank without actually generating them.

To be more specific, let us consider four subsets (boxes) in a Cantor set C^a, depicted in Figure 6.2. They are boxes of size d, and the distance between any two of them is $(1-2a)d$. The interactions between them are of low rank (see section 4.2), and can be represented via scattering matrices (see section 5.3).

Starting with the hierarchical structure of a Cantor set C^a (see section 2.1), we proceed by introducing a set of frame boxes arranged in a tree structure (see section 5.3). For a given precision ϵ, we determine the number of Legendre nodes needed on frame boundaries for the representation of potentials (see Tables 5.1 and 5.2). Then we precompute the inverses of operators P_d and P_s defined by formulae (5.38) and (5.39), via the classical Galerkin method (see section 5.3.1).

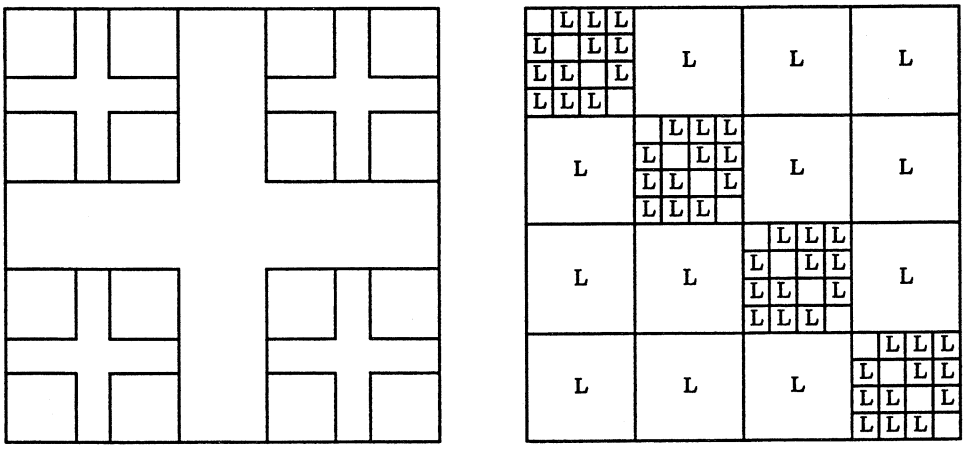

Figure 6.1: Approximation of Cantor set and Coefficient Matrix

To describe the algorithm, we need the following notation.

L Number of levels in the approximation of the Cantor set C^a.

N $N = 4^L$, the size of the approximation of the Cantor set C^a

p The number of Legendre nodes on each side of frame boundaries for the representation of potentials to a given precision ϵ

L_1 The number of a level on which a scattering matrix is computed directly.

m $= 4^{L-L_1}$, size of linear systems to be solved directly

A_f The $m \times m$ matrix A_f is the restriction of matrix A in (2.11) onto a subset ($ibox$) at level L_1. In other words, $(A_f)_{ij} = \ln ||z_i - z_j||$, and $(A_f)_{ii} = L \ln a + \delta$, where points $\{z_1, \cdots, z_m\} \subset ibox$, and δ is a constant.

The fast direct algorithm is a two-pass procedure. In the first (bottom-up) pass, we compute the scattering matrix for level L_1 directly by using formula (5.43), and scattering matrices for all coarser levels (level number $< L_1$) by using the merging scheme described in Theorem 5.7. In the second (top-down) pass, we generate total incoming potentials on frame boundaries up to level L_1 by using Lemma 5.4. Finally, we solve 4^{L_1} small-scale linear systems of size $m \times m$ directly at level L_1.

Following is a formal description of the algorithm.

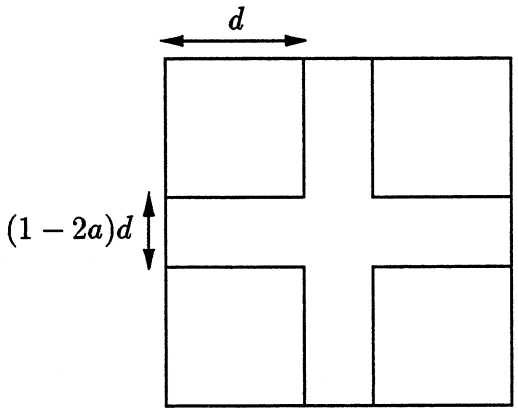

Figure 6.2: Four Subsets of Cantor set C^a

The Algorithm

Initializaiton

Comment [Computations in the initialization are done once for all.]

Step 1

Comment [Given a real number a $(0 < a < \frac{1}{2})$ and an integer L, construct the approximation of Cantor set C^a, and its frame boxes]

do $lev = 0, 1, 2, \cdots, L$

  do $ibox = 1, 2, \cdots, 4^{lev}$

    Divide each box into four corner boxes according to the constant a.

    Construct the frame box for $ibox$ (section 5.3).

  endo

endo

do $lev = L$

  do $ibox = 1, 2, \cdots, 4^L$

    Compute the center of $ibox$.

  enddo

enddo

Step 2

Comment[For a given precision ϵ, precompute operators P_d^{-1}, P_s^{-1}, and A_f^{-1}]
do

Determine number of Legendre nodes p (see Tables 5.1 and 5.2)

Generate the inverses of operators P_d and P_s defined in (5.38) and (5.39), via the classical Galerkin method.

Compute the inverse of $m \times m$ matrix A_f directly.

enddo

Upward Pass

Comment[Compute scattering matrices and splitting matrices]

Step 3

do $lev = L_1$

Compute the discretized operators L and S defined by (5.42) and (5.29).

Compute the scattering matrix directly via formula (5.43): $\alpha = SA_f^{-1}L$.

endo

Step 4

do $lev = L_1 - 1, L_1 - 2, \cdots, 1, 0$

do $i = 1, \cdots, 4$

Compute operators L_i and S_i (defined by formulae (5.45) and (5.48)) via the Gaussian quadrature rule based on Legendre nodes.

do $j = 1, \cdots, 4$

Compute L_{ij} defined by (5.49) via the Gaussian quadrature rule.

endo

endo

Compute the splitting matrix S_p by using formula (5.50).

Compute the scattering matrix α via the merging scheme in Theorem 5.7.

endo

Downward Pass

Comment[Splitting matrices are now available. Compute total incoming potentials on all frame boundaries up to level L_1]

Step 5

do $lev = 1, 2, \cdots, L_1$

  do $ibox = 1, 2, \cdots, 4^{lev}$

    Compute total incoming potential φ_i by means of Lemma 5.4.

  enddo

endo

Step 6

do $ibox = 1, 2, \cdots, 4^{L_1}$

  Solve $m \times m$ linear system directly by computing $\sigma_i = A_f^{-1} L \varphi_i$,

  where operator L is computed at Step 3.

endo

Remark 6.1 *Suppose that ibox is a fixed box at level l. Then in the splitting process, the total incoming potential on the the frame boundary of ibox can be computed independently from those on the other frame boundaries of boxes at the same level.*

Thus, we can obtain a part of the solution independently from the rest of the solution if only a part of the solution is desired.

A brief analysis of the algorithmic complexity is given below.

Step Number	Operation Count	Explanation
1	$O(N)$	$4N$ boxes (squares) are involved. Each box is determined by its center and size.
2	$O(m^3 + p^3)$	Operators P_d and P_s are of size $4p \times 4p$, and the Operator A_f is of size $m \times m$.
3	$O(mp + m^2p)$	Operator L is of size $m \times 4p$. Operator S is of size $4p \times m$. Operator A_f^{-1} is of size $m \times m$.
4	$O(p^3 \log N)$	Operator L_i, S_i, and L_{ij} is of size $4p \times 4p$. S_p is of size $16p \times 4p$. Operator α is of size $4p \times 4p$. There are $\log N$ levels.
5	$O(p^3N)$	The computation of the total incoming potential φ_i on each frame boundary requires p^3 operations. There are 4^{L_1+1} $(< N)$ frame boundaries involved.
6	$O(m^2pN)$	Operator A_f^{-1} is of size $m \times m$. Operator L is of size $m \times 4p$. Potential φ_i is a vector of size $4p$. Computations of $A_f^{-1}L\varphi_i$ are done $4^{L_1}(< N)$ times.

The time complexity of the algorithm is therefore

$$(\beta_1 p^3 + \beta_2 m^2 p) \cdot N + \beta_3 p^3 \cdot \log N, \tag{6.1}$$

where the constant m is normally chosen to be $m \sim 256$, and the constant p depends on the geometry of a given fractal boundary, and the choice of frame boundaries (see Tables 5.1 and 5.2), and the constants β_1, β_2, and β_3 depend on the computer system, implementation, language, etc.

Remark 6.2 *Given scattering matrices and total incoming potentials, the evaluation of the potential*

$$\Psi(x) = \int_{C^a} \ln ||x - t|| d\sigma(t) \tag{6.2}$$

at any point $x \in R^2 \backslash C^a$ requires at most $O(\log N)$ operations, where σ is the charge distribution over C^a.

Chapter 7

Numerical Experiments

We have implemented the fast direct algorithm of the preceding section in Fortran 77. The program is capable of computing either whole or part of the solution, and of evaluating potential at any point. We used our algorithm to compute the harmonic measure on Cantor sets with the dimension of support of harmonic measure determined via the entropy of a set of charges distributed on a Cantor set, the charges representing the solution of the Laplace equation with unity as the boundary condition on that Cantor set.

We will need the following terminology to describe our numerical experiments.

1. **Hausdorff dimension** of Cantor set C^a is given by the formula

$$D = \log 4 / \log(\frac{1}{a}). \tag{7.1}$$

2. **Dimension of Support** of harmonic measure on C^a is given by the formula

$$d = H / \log(\frac{1}{a}), \tag{7.2}$$

where H is the entropy of the system.

3. Approximation of **entropy** H

$$H = \lim_{N \to \infty} H_N \tag{7.3}$$

where

$$H_N = -\frac{1}{N}\sum_{i=1}^{N}\sigma_i \cdot \log \sigma_i \tag{7.4}$$

with $\{\sigma_i\}$ the scaled charge distribution over the system ($\sum_{i=1}^{N}\sigma_i = 1$).

We considered fractal boundaries of Cantor type with ratio 0.1, 0.3, and 0.45. For the first two experiments ($a = 0.1, 0.3$), the potentials on frame boundaries are represented to double precision while they are represented to 10 digits for the third experiment ($a = 0.45$). The size of linear systems inverted directly at the final stage has been chosen to be $m = 256$. The constant δ in the coefficient matrix A defined by formula (2.11) is chosen to be

$$\delta = \frac{\iint_\Omega \ln(\sqrt{(x-x_0)^2+(y-y_0)^2})dxdy}{\iint_\Omega dxdy}, \tag{7.5}$$

where Ω is a square centered at (x_0, y_0) on the finest level of the recursive generation of L-th approximation of Cantor set C^a (see section 2.1). All calculations have been conducted on a Sparc II workstation.

The results are summarized in tables 7.1, 7.2, 7.3, 7.2, 7.5, and 7.6. In tables 7.1, 7.3, and 7.5, the first column is the size of the approximation to a Cantor set. The second column is the number of levels in the generation of a Cantor set. The third column is the actual CPU time of the fast direct algorithm of the preceding section. The forth column is either the CPU time or estimated CPU time of the combined algorithm: the Conjugate Gradient (CG) algorithm combined with the Fast Multipole Method (FMM) (see [46]). The last column is the estimated timing for the Gaussian Elimination (of course, it is given here only for comparison purposes).

The following observations can be made from Tables 7.1, 7.3, and 7.5.

1. Although our fast algorithm asymptotically requires $O(N)$ operations, the actual running time of the algorithm as observed from the numerical experiments seems to behave like $\log N$, due to the fact that the constant β_3 in formula (6.1) is rather large compared to the constants β_1 and β_2. The constant β_3 in formula

(6.1) can be substantially reduced either by a better choice of frame boundaries, or by improving the representation of potentials .

2. For any $N \geq 4096$, our algorithm is faster than the combined algorithm (the CG method combined with the FMM, see [46]).

3. The performance of our algorithm deteriorates with the increase in ratio a as is expected (see Tables 5.1 and 5.2).

Tables 7.2, 7.4, and 7.6 summarize some of our numerical experiments in which the dimension of support of harmonic measure was computed. The part A of the tables is the computed dimension of the support d. The part B of the tables is the the Richarson extrapolation of the first order in terms of levels by the formula

$$d = \frac{md_m - nd_n}{m - n} \tag{7.6}$$

with d_m and d_n the dimensions of support at levels m and n respectively. The part C of the tables is the Richarson extrapolation of the second order in terms of levels defined by the formula

$$d = \frac{m^2 d_{m,l} - n^2 d_{l,n}}{m^2 - n^2} \tag{7.7}$$

with $d_{m,l}$ and $d_{l,n}$ the extrapolated dimensions of support defined by formula (7.6). The following observations can be made from Tables 7.2, 7.4, and 7.6.

1. The dimension of the support of harmonic measure converges linearly with the number of levels.

2. Despite numerical problems often associated with the type of Richarson extrapolation described above (see [50]), the experiments did show reasonable convergence rates: the first order extrapolation in Table 7.4 is consistent with Carleson theorem (see [12]). However, the situation has to be analyzed carefully.

3. Even though our fast algorithm permits simulations on a very large scale to be performed, the field being investigated clearly could benefit from the application

of supercomputers, and possibly parallel machines. Investigation of parallel implementations of algorithms of the type described above will be reported at a later date.

For illustration, the dimension of support is plotted as the function of the Hausdorff dimension in Figures 7.4, 7.5, 7.7, and 7.7. Charge distributions are also plotted in Figures 7.8, 7.9, and 7.10 along the horizontal lines on which the charges are located.

Remark 7.1 *The value (7.5) of the constant δ has been chosen empirically, and no claim is made here as to its optimality.*

The following is a recapitulation of the other notation to be used in the illustration of our numerical experiments.

- a — ratio for generating a Cantor set.
- p — number of Legendre nodes on each side of frame boundaries.
- m — size of linear systems inverted directly.
- ϵ — precision to which incoming and outgoing potentials are represented.
- L — number of levels in the approximation of a Cantor set.
- N — size of the linear system (2.10) to be solved, $N = 4^L$.

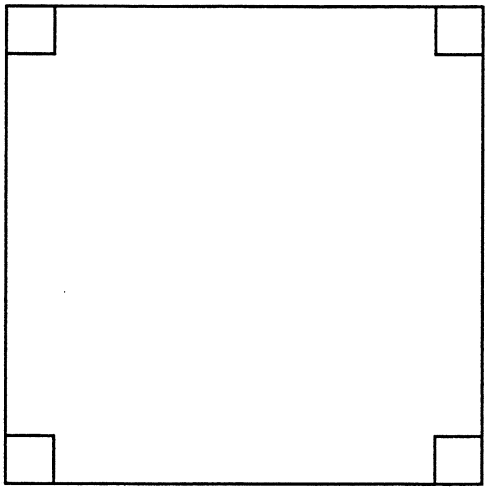

Figure 7.1: Cantor Set with $a = 0.1$

Example 7.1 *Harmonic Measure on Cantor Set C^a with Ratio $a = 0.1$.*

a $= 0.1$, $p = 30$, $m = 256$, $\epsilon = 10^{-14}$

N	Levels	T_{alg}(Minutes)	$T_{CG\&FMM}$(Hours)	T_{GE} (Estimated)
4,096	6	6	0.4	19.1 Hours
16,384	7	9	3.3	51 Days
65,536	8	11	26.4 (est.)	9 years
262,144	9	14	211.2 (est.)	572 years
1,048,576	10	19	1689.6 (est.)	366283 years

Table 7.1: Comparison of Timings ($a = 0.1$)

Hausdorff Dimension $D = 0.602059991327962E + 00$

(A)

Level Number L	Dimension of Support d
6	0.599329045439459E+00
7	0.599189754023720E+00
8	0.599085067779161E+00
9	0.599003595888791E+00
10	0.598938407116325E+00

First Order Extrapolation

(B)

Level Number L	Dimension of Support d
6,7	0.598354005529286E+00
7,8	0.598352264067248E+00
8,9	0.598351820765831E+00
9,10	0.598351708164130E+00

Second Order Extrapolation

(C)

Level Number L	Dimension of Support d
6,7,8	0.598347039681135E+00
7,8,9	0.598350269210872E+00
8,9,10	0.598351257757325E+00

Table 7.2: Dimension of Support d on Cantor Set C^a with $a = 0.1$

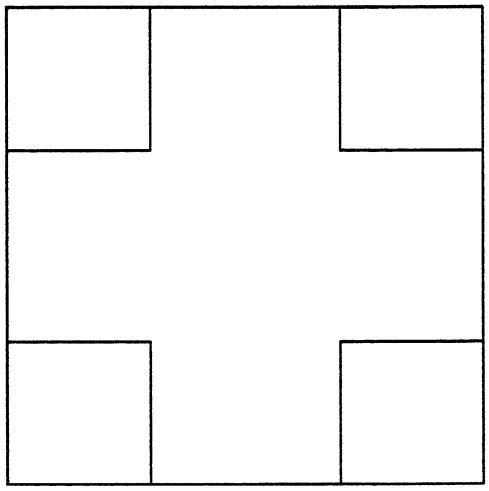

Figure 7.2: Cantor Set with $a = 0.3$

Example 7.2 *Harmonic Measure on Cantor Set C^a with Ratio $a = 0.3$.*

a = 0.3, $p = 60$, $m = 256$, $\epsilon = 10^{-14}$

N	Levels	T_{alg}(Minutes)	$T_{CG\&FMM}$(Hours)	T_{GE} (Estimated)
4,096	6	45	1.2	19.1 Hours
16,384	7	67	8.3	51 Days
65,536	8	88	66.7(est.)	9 years
262,144	9	110	533.8(est.)	572 years
1,048,576	10	134	4270.3(est.)	366283 years

Table 7.3: Comparison of Timings ($a = 0.3$)

Hausdorff Dimension $D = 0.115143328498689E + 01$

(A)

Level Number L	Dimension of Support d
6	0.102592656926789E+01
7	0.101715537867085E+01
8	0.101051673123065E+01
9	0.100533476169737E+01
10	0.100118336944343E+01

First Order Extrapolation

(B)

Level Number L	Dimension of Support d
6,7	0.964528235088610E+00
7,8	0.964046199149250E+00
8,9	0.963879005431130E+00
9,10	0.963820839157970E+00

Second Order Extrapolation

(C)

Level Number L	Dimension of Support d
6,7,8	0.962600091331170E+00
7,8,9	0.963293827417710E+00
8,9,10	0.963588174065331E+00

Table 7.4: Dimension of Support d on Cantor Set C^a with $a = 0.3$

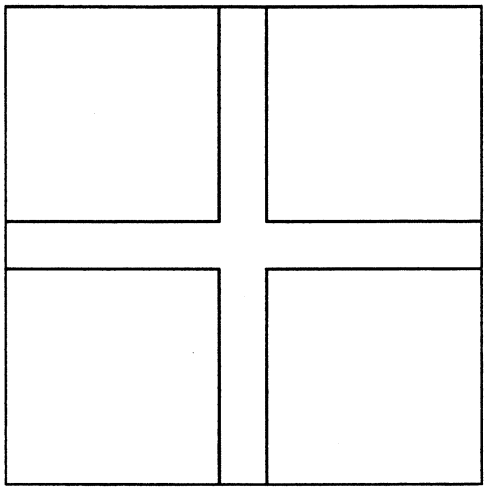

Figure 7.3: Cantor Set with $a = 0.45$

Example 7.3 *Harmonic Measure on Cantor Set C^a with Ratio $a = 0.45$.*

a $= 0.45$, $p = 80$, $m = 256$, $\epsilon = 10^{-10}$.

N	Levels	T_{alg}(Minutes)	$T_{CG\&FMM}$(Hours)	T_{GE} (Estimated)
4,096	6	122	1.6	19.1 Hours
16,384	7	181	13.0	51 Days
65,536	8	240	103.7(est.)	9 years
262,144	9	297	829.3(est.)	572 years
1,048,576	10	360	6634.2(est)	366283 years

Table 7.5: Comparison of Timings ($a = 0.45$)

Hausdorff Dimension $D = 0.173610644917543E + 01$

(A)

Level Numbers	Dimension of Support
6	0.122269892939995E+01
7	0.119171383040669E+01
8	0.116808624449636E+01
9	0.114954943391115E+01
10	0.113465307668069E+01

First Order Extrapolation

(B)

Level Number L	Dimension of Support d
6,7	0.100580323644713E+01
7,8	0.100269314312405E+01
8,9	0.100125494922947E+01
9,10	0.100058586160655E+01

Second Order Extrapolation

(C)

Level Number L	Dimension of Support d
6,7,8	0.993362863154809E+00
7,8,9	0.996221270598445E+00
8,9,10	0.997909511114859E+00

Table 7.6: Dimension of Support d on Cantor Set C^a with $a = 0.45$

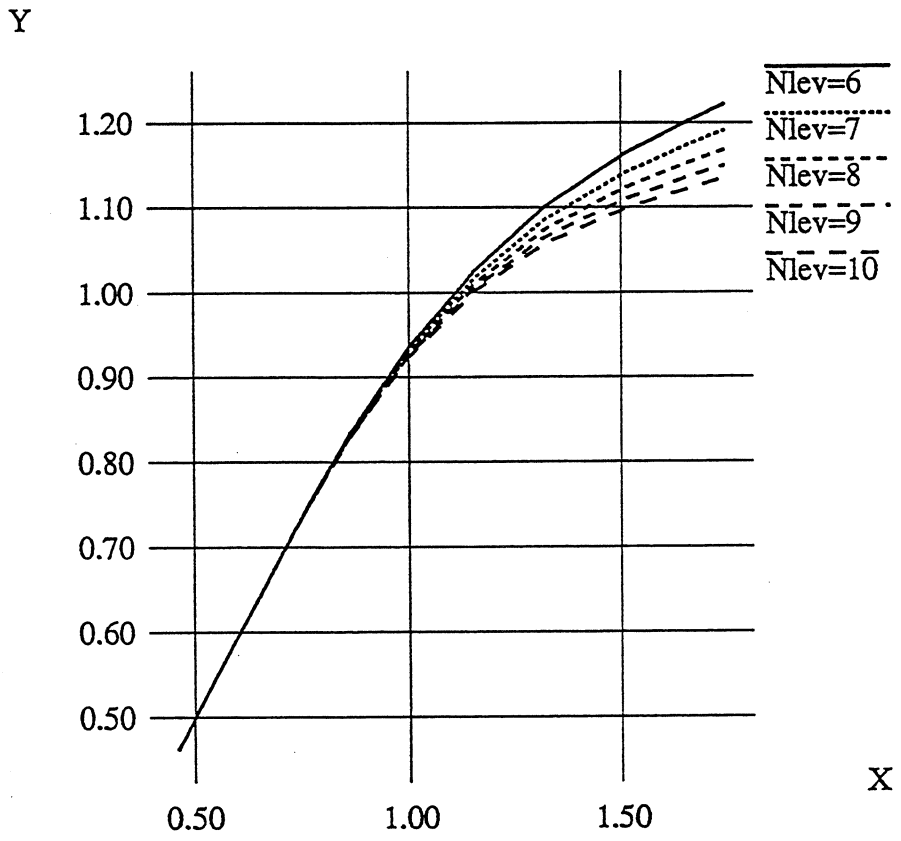

Figure 7.4: Dimension of Support d vs. Hausdorff Dimension D

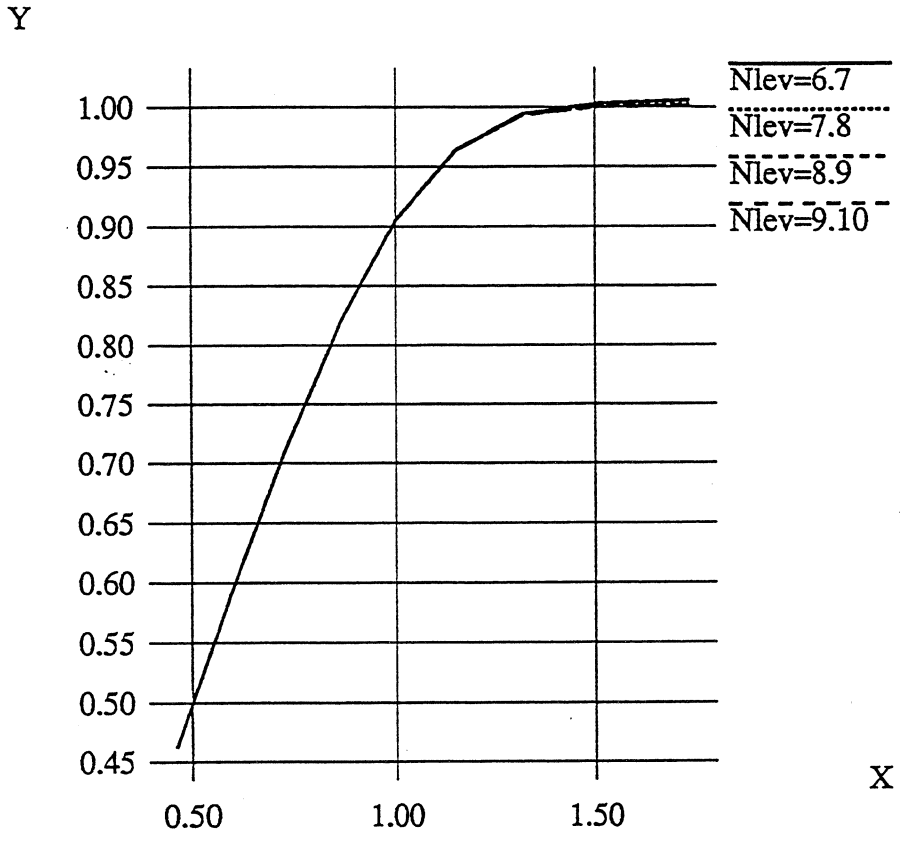

Figure 7.5: Dimension of Support d vs. Hausdorff Dimension D

(First Order Extrapolation)

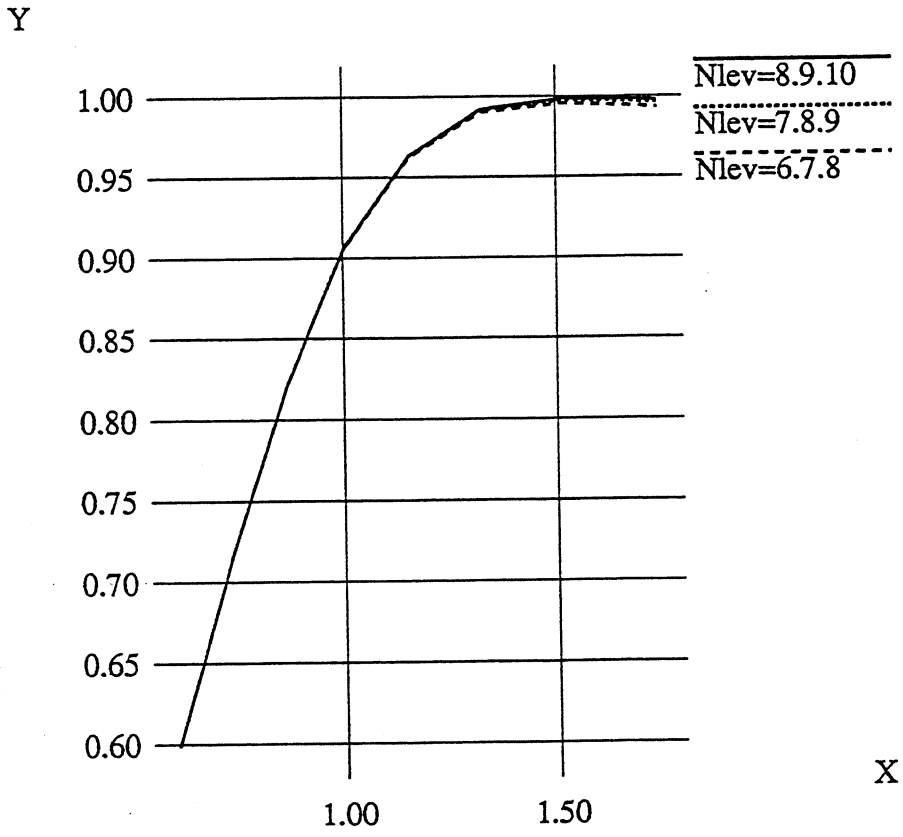

Figure 7.6: Dimension of Support d vs. Hausdorff Dimension D

(Second Order Extrapolation)

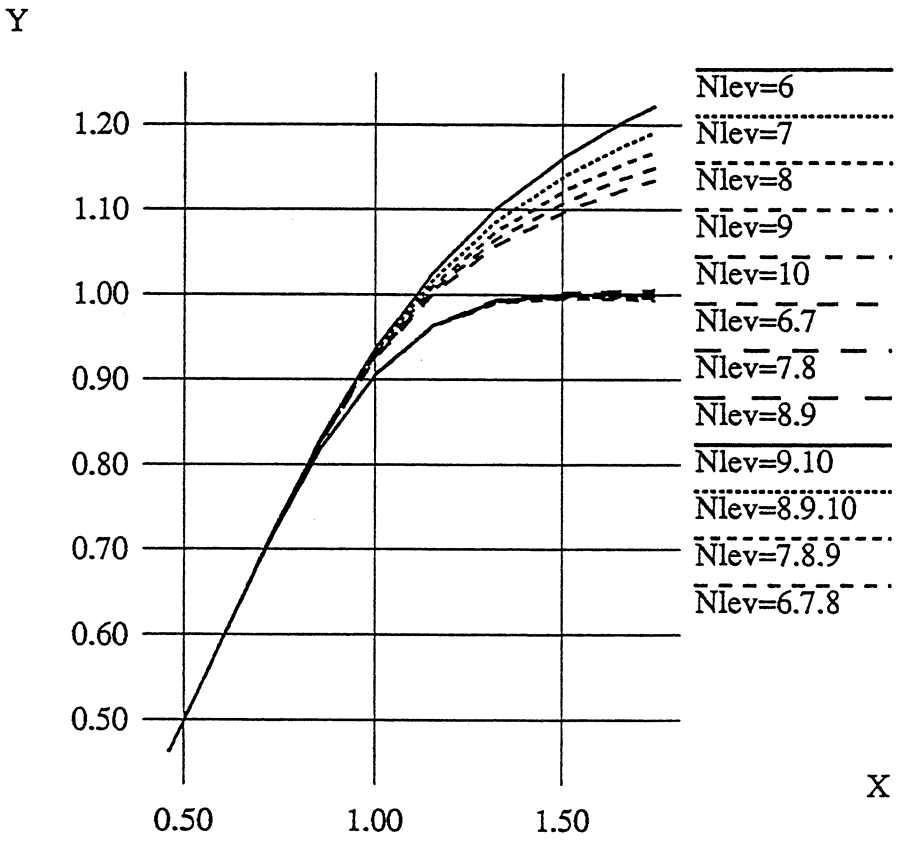

Figure 7.7: Dimension of Support d vs. Hausdorff Dimension D

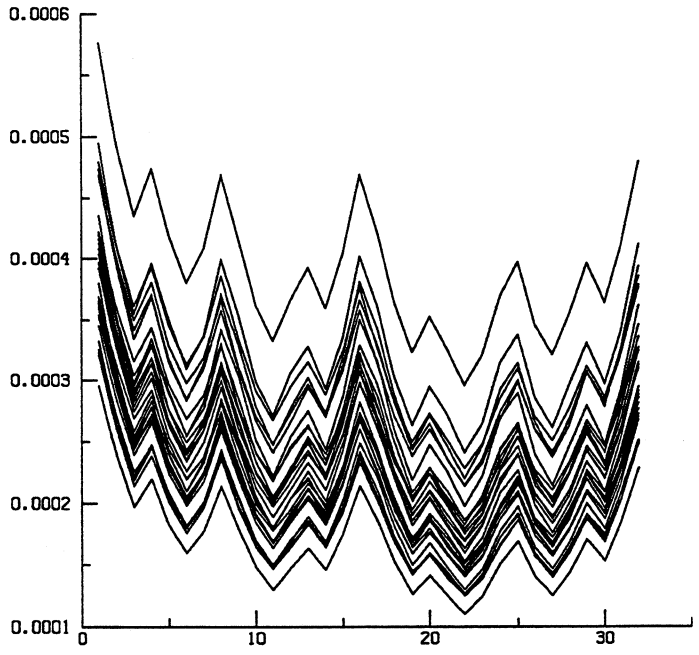

Figure 7.8: Charge Distribution for $a = 0.1$ ($N = 4096$)

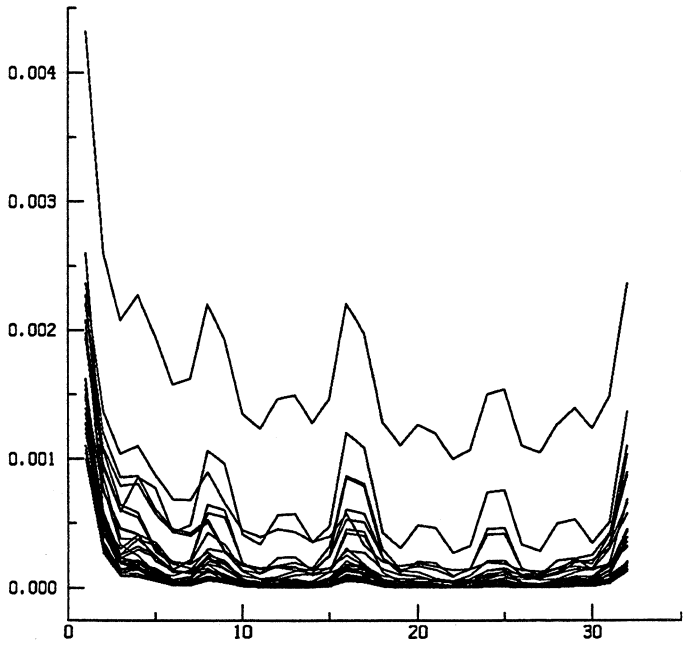

Figure 7.9: Charge Distribution for $a = 0.3$ ($N = 4096$)

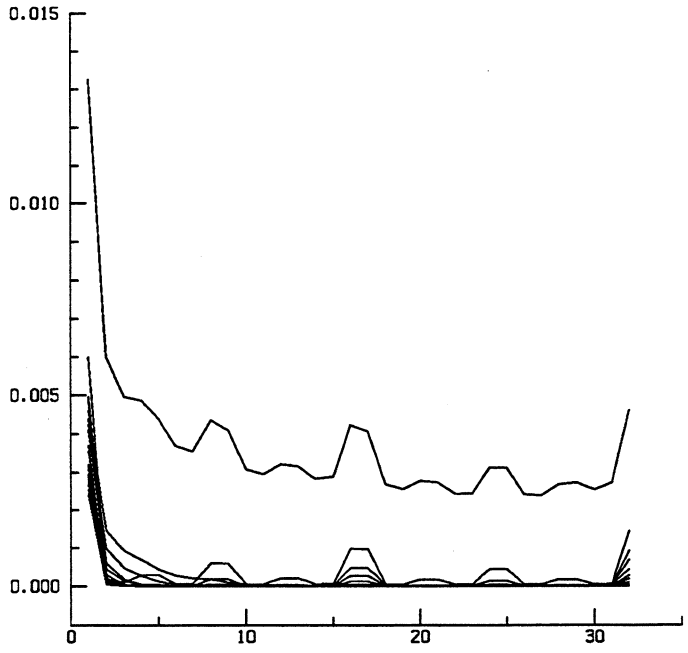

Figure 7.10: Charge Distribution for $a = 0.45$ ($N = 4096$)

Chapter 8

Conclusions and Generalizations

We have presented an $O(N)$ direct algorithm for the rapid solution of the Laplace equation on regions with fractal boundaries. In the algorithm, operators of low rank are recursively compressed, and the inverse is constructed in a compressed form so that it can be applied to a vector rapidly. The algorithm is capable of generating only a part of the solution if desired. The evaluation of potential at any point requires $O(\log N)$ operations.

The fast direct algorithm of this thesis admits far-reaching generalizations. Following are some of the examples.

Harmonic Measure On Cantor Sets In Three Dimensions

It is straightforward to generalize the algorithm of this thesis to solve the Laplace equation in three dimensions on regions with fractal boundaries. In R^3, the behavior of harmonic measure for Cantor sets is completely unknown. Peter Jones recently raised a question about the determination of the actual values of the dimension of the support of harmonic measure on fractals of certain types in R^2, and conjectured that the dimension of the support in R^3 should be always less than two ([34]). The numerical experiments for the computation of harmonic measure in two dimensions would provide experience and insights for the study of harmonic measure on fractals in three dimensions, and eventually

might lead to the understanding of harmonic measure on porous surfaces.

Integral Equations On Fractals

In growth phenomena such as crystallization, electrodeposition, viscous fingering, and diffusion-limited aggregation, the harmonic measure governs the growth of the fractal surfaces, in addition to describing the distribution of growth probabilities ([56]).

A minor modification of the algorithm of this thesis can be used to study the metric properties of harmonic measure on other types of fractals.

Integral Equations with Other Non-Oscillatory Kernels

It is easy to see that the algorithm of this thesis does not substantially depend on the fact the kernel in the integral equation being solved satisfies the Laplace equation. The property of the kernel being used is simply its smoothness away from the diagonal, and the fact that it is non-oscillatory. Thus, the algorithm of this thesis can be generalized to a wide class of integral equations both in two and three dimensions. This work is in progress and will be reported at a later date.

Integral Equations On Curves in R^2 and R^3

One of the approaches to the computation of electrostatic fields in the design of chips and circuits is to formulate the problems as integral equations on curves either in R^2 or R^3 with a free-space Green's function as the kernel (see [59] and [47]). The algorithm of this thesis can be generalized to include fast algorithms for problems of this type. The new algorithms would have advantages over the conventional methods (such as moment method, and finite element method) both in the CPU time requirements, and the accuracy of the solution.

Bibliography

[1] M. Abramowitz and I. A. Stegun, ed., *Handbook of mathematical functions*, National Bureau of Standards, Applied Mathematics Series 55, 1964.

[2] B. Alpert, *Sparse Representation of Smooth Linear Operators*, PhD Thesis, Yale University, December, 1990.

[3] B. Alpert and V. Rokhlin, *A fast Algorithm for the Evaluation of Legendre Expansions*, SIAM J. Sci. Stat. Comput., 12:158-179 (1991).

[4] B. Alpert, G. Beylkin, R. Coifman, and V. Rokhlin, *Wavelets for the Fast solution of Second-Kind Integral Equations*, Technical Report 837, Yale University, Department of Computer Science, 1990.

[5] E. Aurell, M. Benedicks, P. Jones, and S. Grossman, *Harmonic Meausre on a Fractal*, the Annual Review of Swedish Naional Research Council, May, 1992.

[6] O. Axelsson, *Finite Element Solution of Boundary Value Problems: Theory and Computation*, Academic Press, 1984.

[7] M. Barnsley, *Fractals Everywhere*, Academic Press, Inc., 1988.

[8] G. Beylkin, R. Coifman, and V. Rokhlin, *Fast Wavelet Transforms and Numerical Algorithms I*, Communications on Pure and Applied Mathematics, 14:141-183 (1991).

[9] P. Billingsley, *Ergodic Theory and Information*, John Wiley & Sons, Inc., New York-London-Sydney, 1965

[10] G. Birkhoff, and R. Lynch, *Numerical Solution of Elliptic Problems.*

[11] J. Carrier, L. Greengard and V. Rokhlin, *A Fast Adaptive Multipole Algorithm for Particle Simulations*,

[12] L. Carleson, *On the Support of Harmonic Measure for Sets of Cantor Type*, Ann. Acad. Sci. Fenn., 10(1985), 113-123.

[13] R. Courant and D. Hilbert, *Methods of Mathematical Physics, volume II*, Wiley Interscience, New York, 1953.

[14] L. Delves and J. Mohamed, *Computational methods for integral equations*, Cambridge University Press, 1985.

[15] J. L. Doob, *Classical Potential Theory and Its Probabilistic Counterpart*, Springer-Verlag, New York, 1983.

[16] G. A. Edgar, *Measure, Topology, and Fractal Geometry*, Springer-Verlag New York Inc., 1990.

[17] K. J. Falconer, *The Geometry of Fractal Sets*, Cambridge University Press, 1985.

[18] S. Fisher, *Function Theory on Planar Domains*, John Wiley & Sons, New York, 1983.

[19] H. Federer, *Geometric Measure Theory*, Springer, New York, 1969.

[20] C. A. J. Fletcher, *Computational Galerkin Methods*, Springer-Verlag, New York, 1984.

[21] W. Fuchs, *Topic in the Theory of Functions of One Complex Variable*, D. Van Nostrand Company, Inc., Princeton, New Jersey, 1967.

[22] J. Garnett, *Applications of Harmonic Measure*, Jonn Wiley & Sons, New York, 1986.

[23] G. H. Golub and C. F. Van Loan, *Matrix Computations*, Johns Hopkins University Press, 1983.

[24] H. Grandin, *Fundamentals of the Finite Element Method*, Macmillian, New York, 1986.

[25] L. Greengard and V. Rokhlin, *A Fast Algorithm for Particle Simulations*, Journal of Computational Physics, 73:325-348 (1987).

[26] L. Greengard and V. Rokhlin, *On the Numerical Solution of Two-Point Boundary Value Problems*, Communications on Pure and Applied Mathematics, 14:419-452 (1991).

[27] L. Greengard and J. Strain, *The Fast Gauss Transform*, SIAM J. of Sci. and Stat. Comput., 12:79-94 (1991).

[28] P. Henrici, *Applied and Computational Complex Analysis*, Vol. 1, Jonn Wiley & Sons, New York, 1974.

[29] P. Henrici, *Applied and Computational Complex Analysis*, Vol. 3, Jonn Wiley & Sons, New York, 1974.

[30] H. G. Heuser, *Functional Analysis*, John Wiley & Sons, New York, 1982

[31] E. Hille, *Analytic Function Theory*, Vol. II, Chelsea Publishing Company, New York, 1987.

[32] C. Johnson, *Numerical Solution of Partial Differential Equations by the Finite Element Method*, Cambridge Univerisity Press, 1987.

[33] P. Jones and T. Wolff, *Hausdorff Dimension of Harmonic Measures in the Plane* Acta Mathematica, vol. 161, 1988.

[34] P. Jones, Personal Communication.

[35] J. Kelley and T.P. Sirinivasan, *Measure and Integral*, Vol. 1, Springer-Verlag, 1988.

[36] P. Koosis, *The Logarithmic Integral*, Vol.1, Cambridge University Press, Cambridge, 1988.

[37] P. Lax and R. Phillips, *Scattering Theory*, Academic Press, New York, 1967.

[38] N. G. Makarov, *Metric Properties of Harmonic Measure*, Proc. Inter. Cong. Math, Berkeley, California, USA, 1986

[39] B. Mandelbrot, *Fractals: Form, Chance and Dimension* , W. H. Freeman and Co., San Francisco, 1977.

[40] B. Mandelbrot, *The Fractal Geometry of Nature*, W. H. Freeman and Co., San Francisco, 1982.

[41] S. G. Mikhlin, *Integral equations and their applications to certain problems in mechanics, mathematical physics, and technology*, Pergamon Press, 1957.

[42] N. I. Muskhelishvili, *Singular Integral Equations*, Groningen: Wolters-Noordhoff, 1972.

[43] Z. Nehari, *Conformal Mapping*, Dover Publications, Inc., New York, 1975.

[44] I. G. Petrovsky, *Lectures on Partial Differential Equations*, Dover Publications, Inc., New York, 1991.

[45] C. A. Rogers, *Hausdorff Measures*, Cambridge University Press, 1970.

[46] V. Rokhlin, *Rapid Solution of Integral Equations of Classical Potential Theory*, J. Comput. Phys., 60(1985), pp.187-207.

[47] S. Rao, T. Sarkar,, and R. Harrington, The Electrostatic Field of Conducting Bodies in Multiple Dielectric Media, IEEE Trans. on Microswave Theory and Techniques, Vol. MTT-32, N0. 11, Nov., 1984

[48] P. Starr, *On the Numerical Solution of One-Dimensional Integral and Differential Equations*, PhD Thesis, Yale University, May, 1992.

[49] P. Starr and V. Rokhlin, *On the Numerical Solution of Two-Point Boundary Value Problems II*, Technical Report 802, Yale University, Department of Computer Science, 1990, submitted to *Mathematics of Computation.*

[50] J. Stoer and R. Bulirsch, *Introduction to Numerical Analysis*, Springer-Verlag, New York, 1980.

[51] J. Strain, *The Fast Gauss Transform with Variable Scales*, SIAM J. of Sci. and Stat. Comput., 12:1131-1139 (1991).

[52] G. Strang, *Analysis of the Finite Element Method.* Prentice-Hall, Englewood Cliffs, New Jersy, 1973.

[53] B. A. Szabo and I. Babuska, *Finite Element Analysis*, Wiley, New York, 1991.

[54] H. Takayasu, *Fractals in the Physical Sciences*, Manchester University Press, Manchester and New York, 1990

[55] M. Tsuji, *Potential Theory in Modern Function Theory*, Stevens & Co., New York, 1959.

[56] T. Vicsek, *Fractal Growth Phenomena*, World Scientific Publishing Co. Pte. Ltd., 1989.

[57] J. L. Walsh, *Interpolation and Approximation by Rational Functions in the Complex Domain*, Ammerican Mathematical Society Colloquium Publications, vol. 20, 1935.

[58] J. L. Walsh, *The Location of Critical Points of Analytical and Harmonic Functions*, American Mathematical Society Colloquium Publications, vol. 34, 1950.

[59] C. Wei, R. Harrington, J. Mautz, and T. Sarkar, *Multiconductor Transmission Lines in Multilayered Dielectric Media*, IEEE Trans. on Microswave Theory and Techniques, Vol. MTT-32, N0. 4, April, 1984.

[60] J. Wermer, *Potential Theory*, Lecture Notes in Mathematics, No. 408, Springer-Verlag, 1981.

[61] T. Y. Yang, *Finite Element Structural Analysis*, Prentice-Hall, New Jersey, 1986.

Appendix A

Measure Theory

In this appendix, we collect relevant facts in the literature about Borel integration, and harmonic measure. Facts about Borel measure can be found, for example, in [35], and about harmonic measure in [21], [15], [31], and [55].

A.1 Borel Measure and Integration

Definition A.1 *(δ-ring) Let $\mathcal{R}$ be a non-empty family of sets. It is a δ-ring if the following three conditions hold.*

1. *For any sets $A \in \mathcal{R}$ and $B \in \mathcal{R}$,*

$$A \bigcup B \in \mathcal{R}. \tag{A.1}$$

2. *For any sets $A \in \mathcal{R}$ and $B \in \mathcal{R}$,*

$$A \backslash B \in \mathcal{R}. \tag{A.2}$$

3. *For a countable sequence of sets $\{A_n\} \subset \mathcal{R}$,*

$$\bigcap A_n \in \mathcal{R}. \tag{A.3}$$